The Journal of Chemical Physics

Efficient implementation of isotropic cubic response functions for two-photon absorption cross sections within the self-consistent field approximation

Cite as: J. Chem. Phys. **154**, 024111 (2021); https://doi.org/10.1063/5.0031851
Submitted: 05 October 2020 . Accepted: 13 December 2020 . Published Online: 12 January 2021

Karan Ahmadzadeh, Mikael Scott, Manuel Brand, Olav Vahtras, Xin Li, Zilvinas Rinkevicius, and Patrick Norman

The Journal of Chemical Physics ARTICLE scitation.org/journal/jcp

Efficient implementation of isotropic cubic response functions for two-photon absorption cross sections within the self-consistent field approximation

Cite as: J. Chem. Phys. 154, 024111 (2021); doi: 10.1063/5.0031851
Submitted: 5 October 2020 • Accepted: 13 December 2020 •
Published Online: 12 January 2021

Karan Ahmadzadeh,[1,a] Mikael Scott,[2] Manuel Brand,[1] Olav Vahtras,[1] Xin Li,[1] Zilvinas Rinkevicius,[1,3] and Patrick Norman[1,b]

AFFILIATIONS

[1] Department of Theoretical Chemistry and Biology, School of Engineering Sciences in Chemistry, Biotechnology and Health, KTH Royal Institute of Technology, SE-106 91 Stockholm, Sweden

[2] Interdisciplinary Center for Scientific Computing, Ruprecht-Karls University, Im Neuenheimer Feld 205, 69120 Heidelberg, Germany

[3] Department of Physics, Faculty of Mathematics and Natural Sciences, Kaunas University of Technology, Kaunas LT-51368, Lithuania

[a] **Electronic mail:** karana@kth.se
[b] **Author to whom correspondence should be addressed:** panor@kth.se

ABSTRACT

Within the self-consistent field approximation, computationally tractable expressions for the isotropic second-order hyperpolarizability have been derived and implemented for the calculation of two-photon absorption cross sections. The novel tensor average formulation presented in this work allows for the evaluation of isotropic damped cubic response functions using only ~3.3% (one-photon off-resonance regions) and ~10% (one-photon resonance regions) of the number of auxiliary Fock matrices required when explicitly calculating all the needed individual tensor components. Numerical examples of the two-photon absorption cross section in the one-photon off-resonance and resonance regions are provided for alanine–tryptophan and 2,5-dibromo-1,4-bis(2-(4-diphenylaminophenyl)vinyl)-benzene. Furthermore, a benchmark set of 22 additional small- and medium-sized organic molecules is considered. In all these calculations, a quantitative assessment is made of the reduced and approximate forms of the cubic response function in the one-photon off-resonance regions and results demonstrate a relative error of less than ~5% when using the reduced expression as compared to the full form of the isotropic cubic response function.

I. INTRODUCTION

Two-photon absorption (TPA) is a nonlinear optical process with a quadratic dependence on the intensity of the incoming electric field.[1] It has been of high interest in the fields of chemistry and physics where it is used in fundamental studies of electronic structures and in applications such as 3D-microfabrication,[2–5] multi-photon imaging,[6–9] photodynamic therapy,[10,11] optical power limiting,[12,13] and optical data storage.[14] During the past decade, the development of photo-removable protecting groups, or "caging compounds," has been pursued with the aim to achieve targeted drug delivery by means of selective irradiation of damaged tissue and triggered by the TPA process.[15–24] As another very recent application in medicine, we note the promising development of

two-photon fluorescent probes for the diagnosis of Alzheimer's disease, which has been evaluated using theoretical calculations of TPA cross sections.[25]

Theoretical models for spectroscopic properties and particularly TPA cross sections can be used to reveal and analyze microscopic relationships between the electronic structure and the nonlinear optical processes vital to the development of novel two-photon absorbing materials. In computational chemistry, response theory with its long history represents a cornerstone in the development of approximate-state approaches. In 1982, Dalgaard[26] described how quadratic response functions could be evaluated at the time-dependent Hartree–Fock (HF) level of theory. In 1985, Olsen and Jørgensen[27] presented a general formulation of response theory that was further developed by Norman *et al.*[28–31] into a form including a description of relaxation in the system. These formulations utilized the Ehrenfest theorem as the equation of motion for HF or multi-configurational self-consistent field (MCSCF) reference states, and they have given rise to several algorithmic developments and program implementations over the years, and of particular relevance for this work are those concerned with cubic response functions.[32–36] In the conventional formulation of response theory, excited-state and transition-state properties can be retrieved from poles and residues of ground state response functions, whereas the response functions themselves are divergent and unphysical at these resonance frequencies.[27] As an example, one can use the residue of the quadratic response function to obtain two-photon transition amplitudes. In a damped response theory formulation,[28–31] on the other hand, the real and imaginary parts of the response function directly correspond to physical observables and, e.g., TPA cross sections can be identified from the imaginary part of the cubic response function involving electric-dipole operators.

At present, there are several program implementations available for the calculation of TPA spectra. In Dalton,[37] both the quadratic and cubic response theory approaches are available at the density functional theory (DFT) level of theory[36,38] and the former is also available for MCSCF[39] and coupled cluster (CC) wave functions.[40] In Turbomole,[41] the quadratic response theory approach is available at the DFT level of theory,[42] and in Dirac,[43] it is available at the four-component level of DFT.[44,45] At the level of correlated wave-function theory, two-photon transition amplitudes can be calculated with the algebraic diagrammatic construction (ADC) method in the Q-Chem program,[46,47] and additional CC implementations are available in several software packages.[48–51]

In cases when the quadratic and cubic response theory approaches are both applicable, they result in near identical TPA spectra,[36,52,53] so in this situation, it is natural to choose the former over the latter as it is, in general, computationally less expensive. However, the residue-based quadratic response approach is limited to one-photon off-resonance regions of the spectrum and it comes with a need to determine the eigenstates corresponding to the final two-photon states in the absorption process. This is typically achieved with the Davidson algorithm, and it therefore becomes impractical when studying systems with a high density of states, such as large-scale systems, or high-energy regions of the spectrum, such as the soft x-ray region, where the semi-bound two-photon states are found embedded in a continuum of valence-ionized states. In contrast, in the damped cubic response approach, the TPA cross sections are evaluated in an arbitrary frequency range without reference to the underlying eigenstates.

The key reasons as to why the calculation of TPA spectra from the damped cubic response function is computationally expensive are not associated with the fact that response equations become complex *per se* as efficient and stable complex linear response equation solvers have been formulated and implemented,[54,55] not least recently in the VeloxChem program.[56] Instead, they are concerned with the facts that (i) response vectors that depend both linearly and quadratically on the external electric field amplitudes must be determined and (ii) there are a large number of components of the second-order hyperpolarizability tensor (or γ-tensor) that needs to be evaluated and each component involves multiple contractions of generalized Hessian matrices. These computationally demanding steps can both be formulated in terms of constructions of auxiliary Fock matrices from perturbed densities. The specific objectives of the present work are to formulate an algorithm such that a bare minimum of such perturbed Fock matrices needs to be constructed to determine the isotropic average of the imaginary part of the γ-tensor and to the largest degree possible handle these Fock matrix constructions in parallel in the sense that we construct as many as possible from each evaluation of the set of electron-repulsion integrals.

In Sec. II A, we provide the connection between the observable TPA cross section and the microscopic γ-tensor associated with the intensity-dependent refractive index (IDRI) nonlinear optical process and introduce the isotropic average of the latter that is relevant in gas and liquid phases. We further provide the computationally tractable expression for the elements of the γ-tensor in terms of complex cubic response functions and the formulation of contractions of generalized Hessian matrices with response vectors in terms of the above-mentioned perturbed Fock matrices. In Sec. II B, which is the main section of this work, we present novel algorithms for reaching TPA spectrum calculations based on complex cubic response functions that are optimized with respect to Fock matrix constructions. Specifically, in Sec. II B 1, we identify and list the Fock matrices required for the evaluation of the isotropic second-order hyperpolarizability using the method established in the previous implementations.[36,57] This serves as a reference point for the present work, and we are concerned with improvements that go beyond a mere efficient handling of the identified Fock matrices. Most importantly, in Sec. II B 4, we define compounded Fock matrices that minimize the number of matrices that we need to calculate to determine the observable without introducing any approximations (at the given level of electronic structure theory). In Sec. II B 5, we do introduce approximations and form a reduced expression for the isotropic cubic response function that is well motivated for calculations concerned with one-photon off-resonance regions of the spectrum. We note that this is also the by far most important situation as the TPA process can then be separated from multi-step one-photon absorption processes in the experiment. In Sec. II B 6, a tabulated overview of the various schemes that are discussed and developed in this work is provided. Finally, in Sec. III, we provide illustrative TPA spectrum calculations for two separate molecules: first, 2,5-dibromo-1,4-bis(2-(4-diphenylaminophenyl)vinyl)-benzene (BPVB) being a relatively large π-conjugated system and representing a class of two-photon compounds of real technical interest and, second, the alanine–tryptophan (Ala–Trp) diamino acid being a medium-sized

system with a high density of states in the near ultraviolet (UV) region of the spectrum. We examine both the one-photon off-resonance and resonance regions in these calculations.

II. THEORY AND METHODOLOGY

A. Two-photon absorption (TPA) cross sections

1. TPA cross sections and hyperpolarizabilities

Dipoles form in polarizable materials by the induced electric field of incoming light. The resulting polarization can be expanded in a perturbation series in terms of the applied electric field as

$$P_i = \epsilon_0 \chi^{(1)}_{ij} E_j + \epsilon_0 \chi^{(2)}_{ijk} E_j E_k + \epsilon_0 \chi^{(3)}_{ijkl} E_j E_k E_l + \cdots, \tag{1}$$

where $\epsilon_0, \chi^{(1)}, \chi^{(2)}, \chi^{(3)}$, and $\mathbf{E}$ are the electric constant, the linear and non-linear susceptibilities, and the electric field vector, respectively. The energy absorbed by the material per unit volume and time is related to the intensity loss of the electric field as it travels through the material (here in the z-direction),

$$\left\langle \frac{d}{dt}\left(\frac{\text{absorbed energy}}{\text{volume}}\right)\right\rangle = -\frac{dI}{dz} = \sigma^{(1)} I + \sigma^{(2)} I^2 + \cdots, \tag{2}$$

where $\sigma^{(1)}$ and $\sigma^{(2)}$ are the one- and two-photon absorption cross sections, respectively,

$$\sigma^{(1)} = \frac{4\pi\hbar\omega}{nc}\mathrm{Im}\left(\chi^{(1)}(-\omega;\omega)\right), \tag{3}$$

$$\sigma^{(2)} = \frac{24\pi^2\hbar\omega}{n^2c^2}\mathrm{Im}\left(\chi^{(3)}(-\omega;\omega,-\omega,\omega)\right). \tag{4}$$

The bulk susceptibilities $\chi^{(1)}$ and $\chi^{(3)}$ are related to the microscopic (molecular) linear polarizability, α, and second-order hyperpolarizability, γ, through the number density. These molecular properties, in turn, can be derived from response theory as corrections to the expectation value of the electric-dipole moment operator in the presence of an external electric field according to

$$\begin{aligned}\langle\psi(t)|\hat{\mu}_\alpha|\psi(t)\rangle = \langle 0|\hat{\mu}_\alpha|0\rangle &+ \int_{-\infty}^{\infty} \alpha_{\alpha\beta} e^{-i\omega t} E^{\omega}_{\beta}\, d\omega \\ &+ \frac{1}{2}\int_{-\infty}^{\infty}\int_{-\infty}^{\infty} \beta_{\alpha\beta\gamma} e^{-i(\omega_1+\omega_2)t} E^{\omega_1}_{\beta} E^{\omega_2}_{\gamma}\, d\omega_1 d\omega_2 \\ &+ \frac{1}{6}\int_{-\infty}^{\infty}\int_{-\infty}^{\infty}\int_{-\infty}^{\infty} \gamma_{\alpha\beta\gamma\delta} e^{-i(\omega_1+\omega_2+\omega_3)t} \\ &\times E^{\omega_1}_{\beta} E^{\omega_2}_{\gamma} E^{\omega_3}_{\delta}\, d\omega_1 d\omega_2 d\omega_3 + \cdots.\end{aligned} \tag{5}$$

When orientational averaging is taken into consideration [as implied in Eq. (4)], the two-photon absorption cross section can be determined from the isotropic second-order hyperpolarizability defined as

$$\bar{\gamma}(-\omega;\omega,-\omega,\omega) = \frac{1}{15}\sum_{\alpha,\beta}^{x,y,z}\left(\gamma_{\alpha\alpha\beta\beta} + \gamma_{\alpha\beta\alpha\beta} + \gamma_{\alpha\beta\beta\alpha}\right). \tag{6}$$

2. Hyperpolarizabilities and response functions

The second-order hyperpolarizability, $\gamma_{\alpha\beta\gamma\delta}$, as referenced in Eq. (5) is the third-order correction to the expectation value of the dipole moment operator of a molecule in the α direction, $\hat{\mu}_\alpha$, in the presence of a weak external electric field with the oscillation frequencies ω_1, ω_2, and ω_3 that interact with the molecular dipole moments $\hat{\mu}_\beta$, $\hat{\mu}_\gamma$, and $\hat{\mu}_\delta$. The second-order hyperpolarizability can be computed from the cubic response function $\langle\langle\hat{\mu}_\alpha;\hat{\mu}_\beta,\hat{\mu}_\gamma,\hat{\mu}_\delta\rangle\rangle$ and is written in terms of the first-, second-, and third-order response vectors as

$$\begin{aligned}\gamma_{\alpha\beta\gamma\delta}(-\omega_\sigma;\omega_1,\omega_2,\omega_3) &= -\left\langle\left\langle\hat{\mu}_\alpha;\hat{\mu}_\beta,\hat{\mu}_\gamma,\hat{\mu}_\delta\right\rangle\right\rangle_{\omega_1,\omega_2,\omega_3} \\ &= \sum \mathcal{P}_{1,2,3}\Big(\mu^{[1]}_{\alpha} N^{\omega_1,\omega_2,\omega_3}_{\beta,\gamma,\delta} \\ &\quad + \frac{1}{2}\mu^{[2]}_{\alpha}\left(N^{\omega_1,\omega_2}_{\beta,\gamma} N^{\omega_3}_{\delta} + N^{\omega_3}_{\delta} N^{\omega_1,\omega_2}_{\beta,\gamma}\right) \\ &\quad + \mu^{[3]}_{\alpha} N^{\omega_1}_{\beta} N^{\omega_2}_{\gamma} N^{\omega_3}_{\delta}\Big).\end{aligned} \tag{7}$$

The damped response vectors in Eq. (7) are obtained by solving the Ehrenfest equation that yields a set of complex non-Hermitian matrix equations for the first-order (8), second-order (9), and third-order (10) response vectors,

$$N^{\omega_1}_{j;\beta} = \left(E^{[2]} - \omega_1 S^{[2]} - i\gamma R^{[2]}\right)^{-1}_{jk} \mu^{[1]}_{k;\beta}, \tag{8}$$

$$N^{\omega_1,\omega_2}_{j;\beta,\gamma} = \left(E^{[2]} - (\omega_1+\omega_2) S^{[2]} - i\gamma R^{[2]}\right)^{-1}_{jk} \Lambda^{\omega_1,\omega_2}_{k;\beta,\gamma}, \tag{9}$$

$$N^{\omega_1,\omega_2,\omega_3}_{j;\beta,\gamma,\delta} = \left(E^{[2]} - (\omega_1+\omega_2+\omega_3) S^{[2]} - i\gamma R^{[2]}\right)^{-1}_{jk} \Lambda^{\omega_1,\omega_2,\omega_3}_{k;\beta,\gamma,\delta}. \tag{10}$$

The second- and third-order gradient vectors are given by the expressions

$$\Lambda^{\omega_1,\omega_2}_{j;\alpha,\beta} = \mu^{[2]}_{jk;\beta} N^{\omega_1}_{k;\alpha} + \mu^{[2]}_{jk;\alpha} N^{\omega}_{k;\beta} - E^{[3]}_{j(kl)} N^{\omega_1}_{k;\alpha} N^{\omega_2}_{l;\beta}, \tag{11}$$

$$\begin{aligned}\Lambda^{\omega_1,\omega_2,\omega_3}_{j;\beta,\gamma,\delta} = \Big[&\mu^{[3]}_{j(kl),\beta} N^{\omega_2}_{k;\gamma} N^{\omega_3}_{l;\delta} + \mu^{[3]}_{j(kl);\gamma} N^{\omega_1}_{k;\beta} N^{\omega_3}_{l;\delta} + \mu^{[3]}_{j(kl);\delta} N^{\omega_1}_{k;\beta} N^{\omega_2}_{l;\gamma} \\ &- \mu^{[2]}_{jk;\beta} N^{\omega_2,\omega_3}_{k;\gamma,\delta} - \mu^{[2]}_{jk;\gamma} N^{\omega_1,\omega_3}_{k;\beta,\delta} - \mu^{[2]}_{jk;\delta} N^{\omega_1,\omega_2}_{k;\beta,\gamma} E^{[3]}_{j(kl)} \\ &\times \left[N^{\omega_1}_{k;\beta} N^{\omega_2,\omega_3}_{l;\gamma,\delta} + N^{\omega_2}_{k;\gamma} N^{\omega_1,\omega_3}_{l;\beta,\delta} + N^{\omega_3}_{k;\delta} N^{\omega_1,\omega_2}_{l;\beta,\gamma}\right] \\ &- T^{[4]}_{jklm} N^{\omega_1}_{k;\beta} N^{\omega_2}_{l;\gamma} N^{\omega_3}_{m;\delta}\Big],\end{aligned} \tag{12}$$

where we have used the compounded fourth-order tensor defined as

$$\begin{aligned}T^{[4]}_{jklm}(\omega_1,\omega_2,\omega_3) = \Big(&E^{[4]}_{j(klm)} - \omega_1 S^{[4]}_{jk(lm)} - \omega_2 S^{[4]}_{jl(km)} \\ &- \omega_3 S^{[4]}_{jm(kl)} - i\gamma R^{[4]}_{j(klm)}\Big).\end{aligned} \tag{13}$$

The explicit expressions for tensors $E^{[4]}$, $R^{[4]}$, $S^{[4]}$ have been extensively treated previously and are discussed in the work of Olsen and Jørgensen[27] and Norman *et al.*[36,57] Combining the expression for the cubic response function of Eq. (7) and the first- and second-order response vectors of Eqs. (8) and (9) together with the third-order gradient vector of Eq. (12), we obtain the main equation for the cubic response function used in this work,

$$\gamma_{\alpha\beta\gamma\delta}(-\omega;\omega,-\omega,\omega) = -\langle\langle\hat{\mu}_\alpha;\hat{\mu}_\beta,\hat{\mu}_\gamma,\hat{\mu}_\delta\rangle\rangle_{\omega,-\omega,\omega} = N^{-\omega}_{j;\alpha}\left[\mu^{[3]}_{j(kl);\beta}N^{-\omega}_{k;\gamma}N^{\omega}_{l;\delta} + \mu^{[3]}_{j(kl);\gamma}N^{\omega}_{k;\beta}N^{\omega}_{l;\delta} + \mu^{[3]}_{j(kl);\delta}N^{\omega}_{k;\beta}N^{-\omega}_{l;\gamma}\right]$$
$$- N^{-\omega}_{j;\alpha}\left[\mu^{[2]}_{jk;\beta}N^{-\omega,\omega}_{k;\gamma,\delta} + \mu^{[2]}_{jk;\gamma}N^{\omega,\omega}_{k;\beta,\delta} + \mu^{[2]}_{jk;\delta}N^{\omega,-\omega}_{k;\beta,\gamma}\right] + N^{-\omega}_{j;\alpha}E^{[3]}_{j(kl)}\left[N^{\omega}_{k;\beta}N^{-\omega,\omega}_{l;\gamma\delta} + N^{-\omega}_{k;\gamma}N^{\omega,\omega}_{l;\beta,\delta} + N^{\omega}_{k;\delta}N^{\omega,-\omega}_{l;\beta,\gamma}\right]$$
$$- N^{-\omega}_{j;\alpha}T^{[4]}_{jklm}N^{\omega}_{k;\beta}N^{-\omega}_{l;\gamma}N^{\omega}_{m;\delta} + \mu^{[2]}_{(jk);\alpha}\left[N^{\omega}_{j;\beta}N^{-\omega,\omega}_{k;\gamma,\delta} + N^{-\omega}_{j;\gamma}N^{\omega,\omega}_{k;\beta,\delta} + N^{\omega}_{j;\delta}N^{\omega,-\omega}_{k;\beta,\gamma}\right] + \mu^{[3]}_{(jkl);\alpha}N^{\omega}_{j;\beta}N^{-\omega}_{k;\gamma}N^{\omega}_{l;\delta}, \quad (14)$$

where tensor indices in parentheses are permuted. In the present implementation, the coupled equations are solved in separate steps: first, the first-order response vectors are converged, and from these, perturbed Fock matrices required for the construction of the second-order gradients are computed, which are then used to compute the second-order response vectors. Second, these are then used to compute the third-order gradients, which are used to evaluate the cubic response function, avoiding the use of Eq. (10). The $E^{[2]}$ tensors in response equations (8) and (9) quickly become large with increasing system size and are not formed explicitly. Instead, damped response equations (8) and (9) are solved in a reduced subspace, and the details of this procedure are described in the work of Kauczor and Norman.[55]

3. Evaluation of response functions by means of Fock matrices

The contraction of the generalized Hessian tensors $E^{[4]}$ and $E^{[3]}$ in Eq. (14) can be written in terms of transformed Fock matrices without explicit reference to the $E^{[4]}$ and $E^{[3]}$ tensors.[57] The contraction of the $E^{[3]}$ tensor with one first-order response vector and one second-order response vector can be written as

$$E^{[3]}_{j(kl)}N^{\omega_1}_{k;\beta}N^{(\omega_2,\omega_3)}_{l;\gamma,\delta} = -2\begin{bmatrix}\bar{\bar{F}}_{si}\\ -\bar{\bar{F}}_{is}\end{bmatrix}, \quad (15)$$

where i and s refer to occupied and unoccupied orbitals, respectively. The components of the resultant vector can be expressed in terms of one-time transformed first-order Fock matrices of the form $F^{\omega_1}_{\beta}$ [Eq. (27)] and one-time transformed second-order Fock matrices [Eq. (31)] of the form $F^{\omega_1,(\omega_2,\omega_3)}_{\beta,\gamma\delta}$ and the matrix representation of the first- and second-order response vectors $\kappa^{\omega_1}_{\beta}, \kappa^{(\omega_2,\omega_3)}_{\gamma,\delta}$,

$$\bar{\bar{F}} = \zeta^{\omega_1,(\omega_2,\omega_3)}_{\beta,\gamma\delta} + F^{(\beta,\gamma\delta)}, \quad (16)$$

$$F^{(\beta,\gamma\delta)} = F^{\omega_1,(\omega_2,\omega_3)}_{\beta,\gamma\delta} + F^{(\omega_2,\omega_3),\omega_1}_{\gamma\delta,\beta}, \quad (17)$$

$$\zeta^{\omega_1,(\omega_2,\omega_3)}_{\beta,\gamma\delta} = \left[\kappa^{\omega_1}_{\beta},\left[\kappa^{(\omega_2,\omega_3)}_{\gamma,\delta},F_0\right] + 2F^{(\omega_2,\omega_3)}_{\gamma\delta}\right] + \left[\kappa^{(\omega_2,\omega_3)}_{\gamma,\delta},\left[\kappa^{\omega_1}_{\beta},F_0\right] + 2F^{\omega_1}_{\beta}\right]. \quad (18)$$

As can be seen in Eqs. (16)–(18), the contraction of the $E^{[3]}$ tensors with two response vectors exhibits a permutation symmetry with respect to the contracting response vectors. This, as will be seen subsequently, will have consequences for the property gradients that need to be constructed. The $E^{[4]}$ contraction can similarly be expressed in terms of transformed Fock matrices as

$$E^{[4]}_{j(klm)}N^{\omega}_{k;\beta}N^{-\omega}_{l;\gamma}N^{\omega}_{m;\delta} = -2\begin{bmatrix}\bar{\bar{\bar{F}}}_{si}\\ -\bar{\bar{\bar{F}}}_{is}\end{bmatrix}. \quad (19)$$

The Fock matrix $\bar{\bar{\bar{F}}}$ resulting from the contraction of $E^{[4]}$ can be divided into four parts where λ, σ, τ are composed of one-time transformed first-order Fock matrices F^{ω}_{α} and two-time transformed first-order Fock matrices $F^{\omega_1,\omega_2}_{\alpha,\beta}$ [Eq. (28)] and have leading terms that are related to the operators $\hat{\mu}_\beta, \hat{\mu}_\gamma, \hat{\mu}_\delta$ in the cubic response function of Eq. (14). The last term is known as the three-time transformed first-order Fock matrix $F^{(\beta\gamma\delta)}$; see Eq. (29). The total expression takes the form

$$\bar{\bar{\bar{F}}} = \left(\lambda + \sigma + \tau + 3F^{(\beta\gamma\delta)}\right), \quad (20)$$

$$\lambda = \left[\kappa^{\omega}_{\beta},\left[\kappa^{-\omega}_{\gamma},\left[\kappa^{\omega}_{\delta},F\right] + 3F^{\omega}_{\delta}\right] + \left[\kappa^{\omega}_{\delta},\left[\kappa^{-\omega}_{\gamma},F\right] + 3F^{-\omega}_{\gamma}\right] + 3F^{(\gamma\delta)}\right], \quad (21)$$

$$\sigma = \left[\kappa^{-\omega}_{\gamma},\left[\kappa^{\omega}_{\beta},\left[\kappa^{\omega}_{\delta},F\right] + 3F^{\omega}_{\delta}\right] + \left[\kappa^{\omega}_{\delta},\left[\kappa^{\omega}_{\beta},F\right] + 3F^{\omega}_{\beta}\right] + 3F^{(\beta\delta)}\right], \quad (22)$$

$$\tau = \left[\kappa^{\omega}_{\delta},\left[\kappa^{-\omega}_{\gamma},\left[\kappa^{\omega}_{\beta},F\right] + 3F^{\omega}_{\beta}\right] + \left[\kappa^{\omega}_{\beta},\left[\kappa^{-\omega}_{\gamma},F\right] + 3F^{-\omega}_{\gamma}\right] + 3F^{(\beta\gamma)}\right]. \quad (23)$$

The operator indices in parentheses in Eqs. (20)–(22) are permuted with respect to operator and frequency pairs,

$$F^{(\alpha\beta)} = F^{\omega_1,\omega_2}_{\alpha,\beta} + F^{\omega_2,\omega_1}_{\beta,\alpha}, \quad (24)$$

$$F^{(\beta\gamma\delta)} = F^{\omega_1,-\omega_2,\omega_3}_{\beta,\gamma,\delta} + F^{\omega_1,\omega_3,-\omega_2}_{\beta,\delta,\gamma} + F^{-\omega_2,\omega_1,\omega_3}_{\gamma,\beta,\delta} + F^{-\omega_2,\omega_3,\omega_1}_{\gamma,\delta,\beta} + F^{\omega_3,-\omega,\omega_1}_{\delta,\gamma,\beta} + F^{\omega_3,\omega_1,-\omega}_{\delta,\beta,\gamma}. \quad (25)$$

B. Fock matrices in the intensity-dependent refractive index (IDRI) optical process

In this section, we will present the unique sets of Fock matrices that need to be constructed for the evaluation of all the second-order hyperpolarizability tensor components, $\gamma_{\alpha\beta\gamma\delta}$, contained within the isotropic second-order hyperpolarizability $\bar{\gamma}$ of Eq. (6).

1. Complete set of Fock matrices

We start out by identifying the unique first-order response vectors that are required per frequency for the evaluation of the isotropic second-order hyperpolarizability of Eq. (6). Looking at Eqs. (6) and (14), it is evident that three first-order response vectors per frequency are required corresponding to the x, y, and z spatial

components of μ_α. Furthermore, there are response vectors with the same operator but with opposite sign of the optical frequency. The relationship between response vectors with opposite optical frequencies within the self-consistent field (SCF) approximation is given by

$$N_\alpha^\omega = \begin{bmatrix} Z \\ -Y^* \end{bmatrix}, \quad N_\alpha^{-\omega} = \begin{bmatrix} Y \\ -Z^* \end{bmatrix}, \tag{26}$$

which implies that one only needs to solve Eq. (8) for one sign of the optical frequencies and then obtain the reversed signed response vectors by vector manipulation. From the six unique response vectors formed by combining Eq. (26) with response equation (8), six unique one-time transformed first-order Fock matrices can be formed as

$$F_\alpha^\omega = [\kappa_\alpha^\omega, D^0]\mathcal{L}, \tag{27}$$

where κ is the matrix representation of the response vectors of Eq. (26), D^0 is the SCF density matrix, and $\mathcal{L}$ is a matrix containing Coulomb and exchange integrals.[27]

The two-time transformed first-order Fock matrices get their frequency dependence from the first-order response vectors, and their structure is given by

$$F_{\alpha,\beta}^{\omega_1,\omega_2} = \left[\kappa_\alpha^{\omega_1}, \left[\kappa_\beta^{\omega_2}, D^0\right]\right]\mathcal{L}. \tag{28}$$

In general, the two-time transformed first-order Fock matrices do not possess permutation symmetry with respect to the interchange of operators or frequency pairs, which leads to the following set of 27 unique Fock matrices:

$$\left\{(\alpha,\beta) \in \{x,y,z\}, \omega > 0 \,|\, F_{\alpha,\beta}^{\omega,\omega}, F_{\alpha,\beta}^{\omega,-\omega}, F_{\alpha,\beta}^{-\omega,\omega}\right\}.$$

These Fock matrices will later be referenced and used in Eqs. (47)–(49), (53), (54), and (58)–(60).

The three-time transformed first-order Fock matrices get their frequency dependence from the first-order response vectors and are constructed as

$$F_{\alpha,\beta,\gamma}^{\omega_1,\omega_2,\omega_3} = \left[\kappa_\alpha^{\omega_1}, \left[\kappa_\beta^{\omega_2}, \left[\kappa_\gamma^{\omega_3}, D^0\right]\right]\right]\mathcal{L}. \tag{29}$$

They can be found outside the commutators in the $E^{[4]}$ contraction of Eq. (19). Since there are 21 unique $\gamma_{\alpha\beta\gamma\delta}$ tensor components in the isotropic second-order nonlinear hyperpolarizability and the evaluation of each $\gamma_{\alpha\beta\gamma\delta}$ tensor component requires six three-time transformed first-order Fock matrices, the total number of three-time transformed first-order Fock matrices to be computed is 126. However, many of these three-time transformed first-order Fock matrices reoccur and are shared between different tensor components. From Eqs. (66)–(68), where all the three-time transformed first-order Fock matrices have been explicitly written, a set of 21 unique three-indexed first-order Fock matrices can be identified as

$$\left\{(\alpha,\beta) \in \{x,y,z\}, \beta \neq \alpha, \omega > 0 \,|\, F_{\alpha,\alpha,\alpha}^{-\omega,\omega,\omega}, F_{\alpha,\beta,\beta}^{-\omega,\omega,\omega}, F_{\beta,\beta,\alpha}^{-\omega,\omega,\omega}, F_{\beta,\alpha,\beta}^{-\omega,\omega,\omega}\right\}.$$

In addition, the two corresponding sets obtained by permuting the negative frequency with any one of the positive ones are also needed. In total, 63 unique three-indexed first-order Fock matrices are required in order to evaluate the isotropic second-order hyperpolarizability. The unique second-order response vectors required for the computation of the isotropic second-order hyperpolarizability are considered next. These can be identified from Eq. (78) where all the second-order response vectors involved in the $E^{[3]}$ contractions have been written explicitly and are described by the set

$$\left\{(\alpha,\beta) \in \{x,y,z\}, \omega > 0 | N_{\alpha\beta}^{\omega,\omega}, N_{\alpha\beta}^{-\omega,\omega}\right\}.$$

From the second-order gradients of Eq. (11), we see that the gradients exhibit a permutation symmetry with respect to the interchange of the response vectors, which implies that the second order response vectors possess a permutation symmetry with respect to the interchange of the operator and frequency pairs,

$$\Lambda_{\alpha,\beta}^{\omega_1,\omega_2} = \Lambda_{\beta,\alpha}^{\omega_2,\omega_1} \Rightarrow N_{\alpha,\beta}^{\omega_1,\omega_2} = N_{\beta,\alpha}^{\omega_2,\omega_1}. \tag{30}$$

Furthermore, Eq. (30) implies that we get six unique second-order response vectors where both frequencies are positive, $N_{\alpha\beta}^{\omega,\omega}$, since the interchange of α and β yields the same gradient and hence the same second-order response vector. Meanwhile, we get nine unique second-order response vectors of the form $N_{\alpha\beta}^{-\omega,\omega}$ since interchanging α and β does not yield the same second-order gradient since the frequencies now have different signs. Thus, we need to compute 15 second-order response vectors in total.

The one-time transformed second-order Fock matrices are formed from the second-order response vectors as

$$F_{\alpha\beta}^{(\omega_1,\omega_2)} = \left[\kappa_{\alpha\beta}^{(\omega_1,\omega_2)}, D^0\right]\mathcal{L}. \tag{31}$$

The set of unique one-time transformed second-order perturbed Fock matrices can be described by the set

$$\left\{(\alpha,\beta) \in \{x,y,z\}, \omega > 0 | F_{\alpha\beta}^{(\omega,\omega)}, F_{\alpha\beta}^{(\omega,-\omega)}\right\}.$$

As can be seen from Eq. (31), there can only be as many unique one-time transformed second-order Fock matrices as there are unique second-order response vectors; thus, there are in total 15 unique one-time transformed Fock matrices.

The two-time transformed second-order Fock matrices are constructed from one first-order and one second-order response vector as

$$F_{\alpha,\beta\gamma}^{\omega_1,(\omega_2,\omega_3)} = \left[\kappa_\alpha^{\omega_1}, \left[\kappa_{\beta\gamma}^{(\omega_2,\omega_3)}, D^0\right]\right]\mathcal{L}. \tag{32}$$

From the 21 unique γ-tensor components required for the isotropic nonlinear second-order hyperpolarizability, one would in the worst case scenario require 126 two-time transformed second-order Fock matrices since each γ tensor component would require six

two-time transformed second-order Fock matrices [see Eqs. (33) and (34)] where we have explicitly written out all the two-time transformed second-order Fock matrices. Among these 126 two-time transformed second-order Fock matrices, some are however shared between different γ-tensor components, and thus, the unique set of two-time transformed second-order Fock matrices is much smaller. To make the analysis simpler, we separate them based on the frequency of the second-order response vectors involved in the $E^{[3]}$ contraction. The two-time transformed second-order Fock matrices formed using the second-order response vectors with one negative and one positive frequency can be described by the set

$$\Big\{(\alpha,\beta)\in\{x,y,z\},\alpha\neq\beta,\omega>0|F^{\omega,(\omega,-\omega)}_{\alpha,\alpha\alpha},F^{(\omega,-\omega),\omega}_{\alpha\alpha,\alpha},F^{\omega,(\omega,-\omega)}_{\alpha,\beta\beta},F^{(\omega,-\omega),\omega}_{\beta\beta,\alpha},F^{\omega,(\omega,-\omega)}_{\beta,\alpha\beta},F^{(\omega,-\omega),\omega}_{\alpha\beta,\beta}\Big\}.$$

This set is composed of a total of 42 unique Fock matrices. Furthermore, there is another set of Fock matrices of the form $F^{-\omega,(\omega,\omega)}_{\beta,\alpha\beta}$; this set however contains 12 fewer unique Fock matrices since $F^{-\omega,(\omega,\omega)}_{\beta,\alpha\beta}=F^{-\omega,(\omega,\omega)}_{\beta,\beta\alpha}$ due to the second-order gradient symmetry of Eq. (30); these Fock matrices can be described by the set

$$\Big\{(\alpha,\beta)\in\{x,y,z\},\alpha\neq\beta,\omega>0|F^{-\omega,(\omega,\omega)}_{\alpha,\alpha\alpha},F^{(\omega,\omega),-\omega}_{\alpha\alpha,\alpha},F^{-\omega,(\omega,\omega)}_{\alpha,\beta\beta},F^{(\omega,\omega),-\omega}_{\beta\beta,\alpha},F^{-\omega,(\omega,\omega)}_{\beta,\alpha\beta},F^{(\omega,\omega),-\omega}_{\alpha\beta,\beta}\Big\}.$$

Thus, in total, there are 72 unique two-time transformed second-order Fock matrices. In the off-resonance regions where a reduced cubic response equation is applicable [see Eq. (115)], only 30 Fock matrices are required since only the second-order response vectors with two positive frequencies have resonance contributions in these regions.

2. Exploiting Fock matrix linearity

In this section, we will present an algorithm where the linearity of the Fock matrices in the density argument [see Eq. (42)] is used in order to minimize the number of Fock matrices required while retaining all the information about each individual γ-tensor components in the nonlinear second-order hyperpolarizability of Eq. (6). For the two-time transformed first-order Fock matrices, we can add all the permutations in Eqs. (47)–(49), (53), (54), and (58)–(60) while retaining information regarding the individual tensor elements. The set of unique sums of two-time transformed first-order Fock matrices can be described by the set

$$\Big\{(\alpha,\beta)\in\{x,y,z\},\omega>0|\Big(F^{-\omega,\omega}_{\alpha,\beta}+F^{\omega,-\omega}_{\beta,\alpha}\Big),\Big(F^{\omega,\omega}_{\alpha,\beta}+F^{\omega,\omega}_{\beta,\alpha}\Big)\Big\}.$$

There will be nine unique sums of the form $\Big(F^{-\omega,\omega}_{\alpha,\beta}+F^{\omega,-\omega}_{\beta,\alpha}\Big)$ since α and β each make up three different values and interchanging α and β will yield different sums. For the terms of the form $\Big(F^{\omega,\omega}_{\alpha,\beta}+F^{\omega,\omega}_{\beta,\alpha}\Big)$, interchange of α and β yields the same sum such that we get 6 unique sums. Thus, in total, we have 15 unique sums of two-time transformed first-order Fock matrices.

The three-time transformed first-order Fock matrices are obtained from Eqs. (66)–(68), where we have explicitly written out the sums. Since the three-time transformed Fock matrices originating from the $\gamma_{\alpha\alpha\beta\beta}$ components and the $\gamma_{\alpha\beta\beta\alpha}$ components yield the same sums of three-time transformed Fock matrices as can be seen in Eqs. (66) and (67), we obtain the unique contributions from Eqs. (66) and (68). Thus, the unique sums are described by the set

$$\Big\{(\beta,\alpha)\in\{x,y,z\},\omega>0|F^{(\alpha\beta\beta)}_{\alpha},F^{(\beta\alpha\beta)}_{\alpha}\Big\}.$$

The sums of permutations of the three-time transformed Fock matrices of Eqs. (66) and (68) are only equal when $\alpha=\beta$; hence, we get nine unique sums of Fock matrices from each minus three sums of Fock matrices that occur in both expressions for $\alpha=\beta$. Thus, in total, we obtain 15 unique sums of three-time transformed first-order Fock matrices.

One of the constraints for adding second-order response vectors is that they must possess the same frequency arguments such that the matrix to be inverted is the same [see Eqs. (43) and (44)]; thus, one would need to add response vectors from different tensor components in the isotropic gamma tensor; therefore, we cannot use the gradient addition method and retain the individual $\gamma_{\alpha\beta\gamma\delta}$ tensor elements.

Next, we will treat the two-time transformed Fock matrices that are found outside the commutators in the $E^{[3]}$ contraction. Since in total there are 21 unique γ-tensor components in the isotropic cubic response function, we would in the worst-case scenario have 21 unique sums of two-time transformed second-order Fock matrices. However, the terms arising from $\gamma_{\alpha\alpha\beta\beta}$ and $\gamma_{\alpha\beta\beta\alpha}$ are equivalent. Therefore, we get that the sums of two-time transformed second-order Fock matrices that can be added for the $E^{[3]}$ contractions while retaining the individual γ-tensor components can be described by the set

$$\Big\{(\alpha,\beta)\in\{x,y,z\},\omega>0|F^{(\alpha,\beta\beta)},F^{(\beta,\alpha\beta)}\Big\},$$

where

$$F^{(\alpha,\beta\beta)}=F^{(\omega,\omega),-\omega}_{\alpha\beta,\beta}+F^{-\omega,(\omega,\omega)}_{\beta,\alpha\beta}+F^{\omega,(\omega,-\omega)}_{\alpha,\beta\beta}+F^{(\omega,-\omega),\omega}_{\beta\beta,\alpha}+F^{\omega,(\omega,-\omega)}_{\beta,\alpha\beta}+F^{(\omega,-\omega),\omega}_{\alpha\beta,\beta},\tag{33}$$

$$F^{(\beta,\alpha\beta)}=F^{(\omega,\omega),-\omega}_{\beta\beta,\alpha}+F^{-\omega,(\omega,\omega)}_{\alpha,\beta\beta}+F^{\omega,(\omega,-\omega)}_{\beta,\alpha\beta}+F^{\omega,(\omega,-\omega)}_{\beta,\beta\alpha}+F^{(\omega,-\omega),\omega}_{\alpha\beta,\beta}+F^{(\omega,-\omega),\omega}_{\beta\alpha,\beta}.\tag{34}$$

The maximum number of sums we can obtain from each expression in Eqs. (33) and (34) is nine, respectively; however, since the expressions are identical for $\alpha=\beta$, we get that there are three duplicates. Furthermore, there is no symmetry with respect to the interchange of indices α and β in Eqs. (33) and (34) as can be seen from just the two first terms in each equation. Thus, we get a total of 15 unique sums of two-time transformed second-order Fock matrices.

In the off-resonance regions, the only terms that give contributions in Eqs. (33) and (34) are

$$F_{\alpha}^{(\alpha,\beta\beta)} = F_{\alpha\beta,\beta}^{(\omega,\omega),-\omega} + F_{\beta,\alpha\beta}^{-\omega,(\omega,\omega)}, \tag{35}$$

$$F_{\alpha}^{(\beta,\alpha\beta)} = F_{\beta\beta,\alpha}^{(\omega,\omega),-\omega} + F_{\alpha,\beta\beta}^{-\omega,(\omega,\omega)}. \tag{36}$$

For the same reason as in the resonance regions, the number of unique sums of two-time transformed second-order Fock matrices that can be formed for the $E^{[3]}$ contraction while retaining information about individual γ tensor components is 15 per frequency.

3. Subspace extraction

In the optimization scheme developed in this paper, we make full utilization of the subspace procedure for solving the first- and second-order response vectors by constructing Fock matrices used in the third- and fourth-order contractions of the Hessian tensors as linear combinations of the contractions of subspace vectors with the $E^{[2]}$ tensors used in the response equation solver. The one-time transformed first-order Fock matrices can be written in terms of the first-order response vectors as

$$\begin{bmatrix} (F_{\alpha}^{\omega})_{si} \\ -(F_{\alpha}^{\omega})_{is} \end{bmatrix} = E^{[2]} N_{\alpha}^{\omega} - \begin{bmatrix} [\kappa_{\alpha}^{\omega}, F^{0}]_{si} \\ -[\kappa_{\alpha}^{\omega}, F^{0}]_{is} \end{bmatrix}, \tag{37}$$

where the $E^{[2]}$ tensor contraction can be written in terms of the subspace vectors constructed in the symmetrized subspace procedure presented in the work of Kauczor and Norman[55] as

$$E^{[2]}N = \sum_{i=1}^{p} (N_{i,g})_{red}^{R} \bar{f}_{i,g} + \sum_{j=1}^{q} (N_{j,u})_{red}^{R} \bar{f}_{j,u} + i\Big(\sum_{i=1}^{p} (N_{i,g})_{red}^{I} \bar{f}_{i,g} + \sum_{j=1}^{q} (N_{j,u})_{red}^{I} \bar{f}_{j,u}\Big). \tag{38}$$

where the transformed Fock matrix $\bar{f}$ is written in terms of the matrix representation of the vectors that span the subspace, b, as

$$\bar{f} = [b, F^{0}] + [b, D^{0}]\mathcal{L}. \tag{39}$$

In the contraction of the $E^{[3]}$ tensor, all the one- and two-time transformed first- and second-order Fock matrices contained in the ζ term of Eq. (18) can be constructed with no additional computational cost from subspace equations (37) and (38). Likewise, the first-order one-time transformed Fock matrices extracted from the subspace can be used in the terms λ, σ, τ of the $E^{[4]}$ contraction in Eqs. (21) and (22).

4. Compounded Fock matrices for tensor averages

In this section, a novel tensor average algorithm that minimizes the number of Fock matrices and response vectors for the computation of the isotropic second-order hyperpolarizability tensor is presented. Using Eq. (6) and the expression for a single component of the second-order hyperpolarizability tensor [Eq. (14)], the total isotropic second-order hyperpolarizability can be written as

$$\begin{aligned} \bar{\gamma}(-\omega;\omega,-\omega,\omega) = \sum_{\alpha,\beta} \Big(& N_{j;\alpha}^{-\omega} \Big[\Lambda_{k;\alpha,\beta,\beta}^{\omega,-\omega,\omega} + \Lambda_{k;\beta,\beta,\alpha}^{\omega,-\omega,\omega} + \Lambda_{k;\beta,\alpha,\beta}^{\omega,-\omega,\omega} \Big] \\ & + \mu_{(jk);\alpha}^{[2]} \Big[2N_{j;\alpha}^{\omega} N_{k;\beta,\beta}^{-\omega,\omega} + 2N_{j;\beta}^{\omega} \Big(N_{k;\beta,\alpha}^{-\omega,\omega} \\ & + N_{k;\alpha,\beta}^{-\omega,\omega} \Big) + 2N_{j;\beta}^{-\omega} N_{k;\alpha,\beta}^{\omega,\omega} + N_{j;\alpha}^{-\omega} N_{k;\beta,\beta}^{\omega,\omega} \Big] \\ & + \mu_{(jlk);\alpha}^{[3]} \Big[N_{j;\alpha}^{\omega} N_{k;\beta}^{-\omega} N_{l;\beta}^{\omega} + N_{j;\beta}^{\omega} N_{k;\beta}^{-\omega} N_{l;\alpha}^{\omega} \\ & + N_{j;\beta}^{\omega} N_{k;\alpha}^{-\omega} N_{l;\beta}^{\omega} \Big] \Big), \end{aligned} \tag{40}$$

where the symmetry of the second-order response vectors of Eq. (30) has been used to simplify the $\mu^{[2]}$ contraction. All higher order Hessians and response vectors are contained within the third-order gradients of Eq. (40); as such, the first term in the sum is the most computationally demanding contribution to the isotropic second-order hyperpolarizability. Consequently, the remaining parts of this section are devoted to reducing the number of Fock matrices and response vectors contained within the third-order gradients. As seen in the first term of Eq. (40), there exists a unique sum of third-order gradients for every response vector $N_{j;\alpha}^{\omega}$. In order to construct these unique sums of third-order gradients as efficiently as possible, two methods are primarily utilized, namely, density and second-order gradient addition. Pertaining to the first optimization strategy, the transformed Fock matrices can be seen as linear transformations of densities,

$$F(D) = D\mathcal{L}, \tag{41}$$

and the linear nature of the Fock matrix construction from the densities allows for the construction of sums of Fock matrices at the same computational cost of computing an individual Fock matrix,

$$F(D_1) + \cdots + F(D_n) = F(D_1 + \cdots + D_n). \tag{42}$$

The second optimization strategy is the addition of second-order gradients. The matrix that is to be inverted in the linear response equation depends solely on the perturbing frequencies and can be written as

$$N(\Lambda,\omega) = M(\omega)^{-1}\Lambda. \tag{43}$$

This implies that for a given frequency, the response equation is also a linear transformation of the property gradients,

$$N(\Lambda_1,\omega) + \cdots + N(\Lambda_n,\omega) = N(\Lambda_1 + \cdots + \Lambda_n,\omega). \tag{44}$$

Equation (44) allows for the computation of sums of response vectors at the same computational cost as computing a single response vector. In order to make use of Eqs. (42) and (44), the Hessian

contractions formulated within Eq. (40) are reformulated in terms of compounded Fock matrices and compounded response vectors wherever possible. As can be seen in the expression for the $E^{[3]}$ and $T^{[4]}$ contractions [Eqs. (18), (21), and (22)], there exists a recurrence of the one-time transformed first-order Fock matrices required, and all of these Fock matrices can be extracted from the subspace when solving the response equations of Eq. (8) using the subspace extraction scheme developed in Sec. II B 3. The contraction of the $E^{[3]}$ tensors for the second-order hyperpolarizability of Eq. (14), however, also requires the computation of second-order response vectors [Eq. (9)], which require the construction of second-order gradients of the form of Eq. (11), which themselves require $E^{[3]}$ contractions with first-order response vectors. The $E^{[3]}$ contractions within the second-order gradients are constructed from two-time transformed first-order Fock matrices, as can be seen by using Eqs. (15)–(18) with two first-order response vectors. Two-time transformed Fock matrices are also found in the $T^{[4]}$ contraction terms of Eqs. (21) and (22). Thus, the newly defined compounded two-time transformed Fock matrices must be constructed in such a manner that they can be used in both stages. Many of the Fock matrices required for the $T^{[4]}$ contractions are confined within commutators, as can be seen in Eqs. (21) and (22). Thus, one constraint for the application of Eq. (42) is that the leading response matrices in the commutators must be identical such that the two-time transformed first-order Fock matrices within the commutators can be added,

$$\left[\kappa_A^{\omega}, \Theta_1 + F_1\right] + \cdots + \left[\kappa_A^{\omega}, \Theta_n + F_n\right] = \left[\kappa_A^{\omega}, \sum_j^n (\Theta_j + F_j)\right]. \tag{45}$$

One must first note that since the contractions of the $T^{[4]}$ tensor with three single-indexed response vectors yield Fock vectors that are ultimately dotted with vectors of the form $N_{j;\alpha}^{-\omega}$, one would need to separate the resulting Fock vectors based on the α-component of the third-order gradient from Eq. (40). For the $E^{[4]}$ contributions to $\bar{\gamma}$ in Eq. (40) and with further use of Eq. (12), we obtain

$$\begin{aligned}
&\sum_{\alpha,\beta}^{x,y,z} N_{j;\alpha}^{-\omega} E_{j(klm)}^{[4]} \left[N_{k;\alpha}^{\omega} N_{l;\beta}^{-\omega} N_{m;\beta}^{\omega} + N_{k;\beta}^{\omega} N_{l;\alpha}^{-\omega} N_{m;\beta}^{\omega} + N_{k;\beta}^{\omega} N_{l;\beta}^{-\omega} N_{m;\alpha}^{\omega}\right] \\
&\quad = -2 \sum_{\alpha}^{x,y,z} N_{j;\alpha}^{-\omega} \left(\begin{bmatrix} (\lambda^{\alpha\alpha\beta\beta} + \sigma^{\alpha\alpha\beta\beta} + \tau^{\alpha\alpha\beta\beta})_{is} \\ -(\lambda^{\alpha\alpha\beta\beta} + \sigma^{\alpha\alpha\beta\beta} + \tau^{\alpha\alpha\beta\beta})_{si} \end{bmatrix} \right. \\
&\qquad + \begin{bmatrix} (\lambda^{\alpha\beta\alpha\beta} + \sigma^{\alpha\beta\alpha\beta} + \tau^{\alpha\beta\alpha\beta})_{is} \\ -(\lambda^{\alpha\beta\alpha\beta} + \sigma^{\alpha\beta\alpha\beta} + \tau^{\alpha\beta\alpha\beta})_{si} \end{bmatrix} \\
&\qquad \left. + \begin{bmatrix} (\lambda^{\alpha\beta\beta\alpha} + \sigma^{\alpha\beta\beta\alpha} + \tau^{\alpha\beta\beta\alpha})_{is} \\ -(\lambda^{\alpha\beta\beta\alpha} + \sigma^{\alpha\beta\beta\alpha} + \tau^{\alpha\beta\beta\alpha})_{si} \end{bmatrix} + \begin{bmatrix} (F_{\alpha}^{\lambda\sigma\tau})_{is} \\ -(F_{\alpha}^{\lambda\sigma\tau})_{si} \end{bmatrix} \right).
\end{aligned} \tag{46}$$

We will first define and treat the terms in Eq. (46) related to λ. Using the expression for λ in Eq. (21) together with the expression for the isotropic second-order hyperpolarizability [Eq. (40)], we get the three λ contributions corresponding to $\gamma_{\alpha\alpha\beta\beta}$, $\gamma_{\alpha\beta\alpha\beta}$, and $\gamma_{\alpha\beta\beta\alpha}$ as

$$\begin{aligned}
\lambda^{\alpha\alpha\beta\beta} = \sum_{\beta}^{x,y,z} &\left[\kappa_{\alpha}^{\omega}, \left[\kappa_{\beta}^{-\omega}, \left[\kappa_{\beta}^{\omega}, F\right]\right] + 3F_{\beta}^{\omega}\right] + \left[\kappa_{\beta}^{\omega}, \left[\kappa_{\beta}^{-\omega}, F\right] + 3F_{\beta}^{-\omega}\right] \\
&+ 3F_{\beta,\beta}^{-\omega,\omega} + 3F_{\beta,\beta}^{\omega,-\omega}\Big],
\end{aligned} \tag{47}$$

$$\begin{aligned}
\lambda^{\alpha\beta\alpha\beta} = \sum_{\beta}^{x,y,z} &\left[\kappa_{\beta}^{\omega}, \left[\kappa_{\alpha}^{-\omega}, \left[\kappa_{\beta}^{\omega}, F\right]\right] + 3F_{\beta}^{\omega}\right] + \left[\kappa_{\beta}^{\omega}, \left[\kappa_{\alpha}^{-\omega}, F\right] + 3F_{\alpha}^{-\omega}\right] \\
&+ 3F_{\alpha,\beta}^{-\omega,\omega} + 3F_{\beta,\alpha}^{\omega,-\omega}\Big],
\end{aligned} \tag{48}$$

$$\begin{aligned}
\lambda^{\alpha\beta\beta\alpha} = \sum_{\beta}^{x,y,z} &\left[\kappa_{\beta}^{\omega}, \left[\kappa_{\beta}^{-\omega}, \left[\kappa_{\alpha}^{\omega}, F\right]\right] + 3F_{\alpha}^{\omega}\right] + \left[\kappa_{\alpha}^{\omega}, \left[\kappa_{\beta}^{-\omega}, F\right] + 3F_{\beta}^{-\omega}\right] \\
&+ 3F_{\beta,\alpha}^{-\omega,\omega} + 3F_{\alpha,\beta}^{\omega,-\omega}\Big].
\end{aligned} \tag{49}$$

From Eq. (45), we see that provided that the leading response matrices are the same in Eqs. (47)–(49), one can add the two-time transformed Fock matrices within the commutators. To adhere to the constraint of Eq. (45), we divide the sums of Eqs. (47)–(49) into terms where the leading response matrix has an α index and one where the leading response matrix has a β index, where we fix α and let β run through the values x, y and z. To this end, we take the terms where $\alpha = \beta$ from the sums in Eqs. (48) and (49) and add them to Eq. (47) to get the total expression

$$\begin{aligned}
\lambda^{\alpha\alpha\beta\beta} + \lambda^{\alpha\beta\alpha\beta} + \lambda^{\alpha\beta\beta\alpha} = &\left[\kappa_{\alpha}^{\omega}, \sum_{\beta}^{x,y,z} \left(\left[\kappa_{\beta}^{-\omega}, \left[\kappa_{\beta}^{\omega}, F\right]\right] + 3F_{\beta}^{\omega}\right] + \left[\kappa_{\beta}^{\omega}, \left[\kappa_{\beta}^{-\omega}, F\right] + 3F_{\beta}^{-\omega}\right] + 3F_{\beta,\beta}^{-\omega,\omega} + 3F_{\beta,\beta}^{\omega,-\omega} \right) \right. \\
&\left. + 2\left[\kappa_{\alpha}^{-\omega}, \left[\kappa_{\alpha}^{\omega}, F\right]\right] + 3F_{\beta}^{\omega}\right] + 2\left[\kappa_{\alpha}^{\omega}, \left[\kappa_{\alpha}^{-\omega}, F\right] + 3F_{\alpha}^{-\omega}\right] + 6F_{\alpha,\alpha}^{-\omega,\omega} + 6F_{\alpha,\alpha}^{\omega,-\omega} \right] \\
&+ \sum_{\beta\neq\alpha}^{x,y,z} \left(\left[\kappa_{\beta}^{\omega}, \left[\kappa_{\alpha}^{-\omega}, \left[\kappa_{\beta}^{\omega}, F\right]\right] + 3F_{\beta}^{\omega}\right] + \left[\kappa_{\beta}^{\omega}, \left[\kappa_{\alpha}^{-\omega}, F\right] + 3F_{\alpha}^{-\omega}\right] + 3F_{\alpha,\beta}^{-\omega,\omega} + 3F_{\beta,\alpha}^{\omega,-\omega} \right. \\
&\left. + \left[\kappa_{\beta}^{-\omega}, \left[\kappa_{\alpha}^{\omega}, F\right]\right] + 3F_{\alpha}^{\omega}\right] + \left[\kappa_{\alpha}^{\omega}, \left[\kappa_{\beta}^{-\omega}, F\right] + 3F_{\beta}^{-\omega}\right] + 3F_{\beta,\alpha}^{-\omega,\omega} + 3F_{\alpha,\beta}^{\omega,-\omega}\right] \right) \\
= &\sum_{\beta}^{x,y,z} \left[\kappa_{\beta}^{\omega}, \Theta_{\alpha\beta}^{\lambda} + F_{\alpha\beta}^{\lambda}\right],
\end{aligned} \tag{50}$$

where we have introduced the auxiliary matrices

$$\Theta^{\lambda}_{\alpha\beta} = \left[\kappa^{-\omega}_{\alpha}, \left[\kappa^{\omega}_{\beta}, F\right] + 3F^{\omega}_{\beta}\right] + \left[\kappa^{\omega}_{\beta}, \left[\kappa^{-\omega}_{\alpha}, F\right] + 3F^{-\omega}_{\alpha}\right] + \left[\kappa^{-\omega}_{\beta}, \left[\kappa^{\omega}_{\alpha}, F\right] + 3F^{\omega}_{\alpha}\right] + \left[\kappa^{\omega}_{\alpha}, \left[\kappa^{-\omega}_{\beta}, F\right] + 3F^{-\omega}_{\beta}\right] + \delta_{\alpha\beta}\sum_{\rho}^{x,y,z}\left(\left[\kappa^{\omega}_{\rho}, \left[\kappa^{-\omega}_{\rho}, F\right] + 3F^{-\omega}_{\rho}\right] + \left[\kappa^{-\omega}_{\rho}, \left[\kappa^{\omega}_{\rho}, F\right] + 3F^{\omega}_{\rho}\right]\right), \quad (51)$$

$$F^{\lambda}_{\alpha\beta} = 3\left(F^{-\omega,\omega}_{\alpha,\beta} + F^{\omega,-\omega}_{\beta\alpha} + F^{-\omega,\omega}_{\beta,\alpha} + F^{\omega,-\omega}_{\alpha,\beta}\right) + 3\delta_{\alpha\beta}\sum_{\rho}^{x,y,z}\left(F^{-\omega,\omega}_{\rho,\rho} + F^{\omega,-\omega}_{\rho,\rho}\right). \quad (52)$$

$F^{\lambda}_{\alpha\beta}$ in Eqs. (50) and (52) are defined as the two-time transformed compounded first-order Fock matrices that adhere to the commutator density addition constraint of Eq. (45). The first index in $F^{\lambda}_{\alpha\beta}$ refers to that the first index of the gamma tensors whose λ components were added was set to α. The second index in $F^{\lambda}_{\alpha\beta}$ refers to that the second operator in all the gamma tensors added had β. The leading terms of all λ terms get their components from the second operator of the gamma tensor, while the third and fourth operators run through all possible values such that the combination of operators still belongs to the set of gamma tensors that belong to the set of gamma tensors within the isotropic average. For a particular alpha, we can write the expressions for σ in Eq. (46) as

$$\sigma^{\alpha\alpha\beta\beta} = \sum_{\beta}^{x,y,z}\left[\kappa^{-\omega}_{\beta}, \left[\kappa^{\omega}_{\alpha}, \left[\kappa^{\omega}_{\beta}, F\right] + 3F^{\omega}_{\beta}\right] + \left[\kappa^{\omega}_{\beta}, \left[\kappa^{\omega}_{\alpha}, F\right] + 3F^{\omega}_{\alpha}\right] + 3F^{\omega,\omega}_{\alpha,\beta} + 3F^{\omega,\omega}_{\beta,\alpha}\right], \quad (53)$$

$$\sigma^{\alpha\beta\alpha\beta} = \sum_{\beta}^{x,y,z}\left[\kappa^{-\omega}_{\alpha}, \left[\kappa^{\omega}_{\beta}, \left[\kappa^{\omega}_{\beta}, F\right] + 3F^{\omega}_{\beta}\right] + \left[\kappa^{\omega}_{\beta}, \left[\kappa^{\omega}_{\beta}, F\right] + 3F^{\omega}_{\beta}\right] + 3F^{\omega,\omega}_{\beta,\beta} + 3F^{\omega,\omega}_{\beta,\beta}\right], \quad (54)$$

$$\sigma^{\alpha\beta\beta\alpha} = \sum_{\beta}^{x,y,z}\left[\kappa^{-\omega}_{\beta}, \left[\kappa^{\omega}_{\beta}, \left[\kappa^{\omega}_{\alpha}, F\right] + 3F^{\omega}_{\alpha}\right] + \left[\kappa^{\omega}_{\alpha}, \left[\kappa^{\omega}_{\beta}, F\right] + 3F^{\omega}_{\beta}\right] + 3F^{\omega,\omega}_{\beta,\alpha} + 3F^{\omega,\omega}_{\alpha,\beta}\right]. \quad (55)$$

We can then combine all the terms as

$$\begin{aligned}\sigma^{\alpha\beta\alpha\beta} + \sigma^{\alpha\alpha\beta\beta} + \sigma^{\alpha\beta\beta\alpha} &= \Bigg[\kappa^{-\omega}_{\alpha}, \sum_{\beta}^{x,y,z}\left(\left[\kappa^{\omega}_{\beta}, \left[\kappa^{\omega}_{\beta}, F\right] + 3F^{\omega}_{\beta}\right] + \left[\kappa^{\omega}_{\beta}, \left[\kappa^{\omega}_{\beta}, F\right] + 3F^{\omega}_{\beta}\right] + 3F^{\omega,\omega}_{\beta,\beta} + 3F^{\omega,\omega}_{\beta,\beta}\right) \\ &\quad + 2\left[\kappa^{\omega}_{\alpha}, \left[\kappa^{\omega}_{\alpha}, F\right] + 3F^{\omega}_{\alpha}\right] + 2\left[\kappa^{\omega}_{\alpha}, \left[\kappa^{\omega}_{\alpha}, F\right] + 3F^{\omega}_{\alpha}\right] + 12F^{\omega,\omega}_{\alpha,\alpha}\Bigg] \\ &\quad + \sum_{\beta\neq\alpha}^{x,y,z}\Big(\left[\kappa^{-\omega}_{\beta}, \left[\kappa^{\omega}_{\alpha}, \left[\kappa^{\omega}_{\beta}, F\right] + 3F^{\omega}_{\beta}\right] + \left[\kappa^{\omega}_{\beta}, \left[\kappa^{\omega}_{\alpha}, F\right] + 3F^{\omega}_{\alpha}\right] + 3F^{\omega,\omega}_{\alpha,\beta} + 3F^{\omega,\omega}_{\beta,\alpha} \\ &\quad + \left[\kappa^{\omega}_{\beta}, \left[\kappa^{\omega}_{\alpha}, F\right] + 3F^{\omega}_{\alpha}\right] + \left[\kappa^{\omega}_{\alpha}, \left[\kappa^{\omega}_{\beta}, F\right] + 3F^{\omega}_{\beta}\right] + 3F^{\omega,\omega}_{\beta,\alpha} + 3F^{\omega,\omega}_{\alpha,\beta}\right]\Big) \\ &= \sum_{\beta}^{x,y,z}\left[\kappa^{-\omega}_{\beta}, \Theta^{\sigma}_{\alpha\beta} + F^{\sigma}_{\alpha\beta}\right], \end{aligned} \quad (56)$$

where we have introduced the auxiliary matrices

$$\Theta^{\sigma}_{\alpha\beta} = 2\left[\kappa^{\omega}_{\alpha}, \left[\kappa^{\omega}_{\beta}, F\right] + 3F^{\omega}_{\beta}\right] + 2\left[\kappa^{\omega}_{\beta}, \left[\kappa^{\omega}_{\alpha}, F\right] + 3F^{\omega}_{\alpha}\right] + 2\delta_{\alpha\beta}\sum_{\rho}^{x,y,z}\left(\left[\kappa^{\omega}_{\rho}, \left[\kappa^{\omega}_{\rho}, F\right] + 3F^{\omega}_{\rho}\right]\right), \quad (57)$$

$$F^{\sigma}_{\alpha\beta} = 6F^{\omega,\omega}_{\alpha,\beta} + 6F^{\omega,\omega}_{\beta,\alpha} + \delta_{\alpha\beta}\sum_{\rho}^{x,y,z}6F^{\omega,\omega}_{\rho,\rho}.$$

The first index in $F^{\sigma}_{\alpha\beta}$ refers to that the first index in the gamma tensors whose σ components were added was set to α. The second index refers to that the third operator in the added gamma tensors was set to β. The leading terms of all σ terms get their components from the third operator of the gamma tensor [see Eq. (21)], while the second and fourth operators run through all possible values such that the combination of operators still belongs to the set of gamma tensors that exist in the isotropic average. Finally, we now apply Eq. (22) to Eq. (6) and we obtain

$$\tau^{\alpha\alpha\beta\beta} = \sum_{\beta}^{x,y,z}\left[\kappa^{\omega}_{\beta}, \left[\kappa^{-\omega}_{\beta}, \left[\kappa^{\omega}_{\alpha}, F\right] + 3F^{\omega}_{\alpha}\right] + \left[\kappa^{\omega}_{\alpha}, \left[\kappa^{-\omega}_{\beta}, F\right] + 3F^{-\omega}_{\beta}\right] + 3F^{\omega,-\omega}_{\alpha,\beta} + 3F^{-\omega,\omega}_{\beta,\alpha}\right], \quad (58)$$

$$\tau^{\alpha\beta\alpha\beta} = \sum_{\beta}^{x,y,z}\left[\kappa^{\omega}_{\beta}, \left[\kappa^{-\omega}_{\beta}, \left[\kappa^{\omega}_{\beta}, F\right] + 3F^{\omega}_{\beta}\right] + \left[\kappa^{\omega}_{\beta}, \left[\kappa^{-\omega}_{\alpha}, F\right] + 3F^{-\omega}_{\alpha}\right] + 3F^{\omega,-\omega}_{\beta,\alpha} + F^{-\omega,\omega}_{\alpha,\beta}\right], \quad (59)$$

$$\tau^{\alpha\beta\beta\alpha} = \sum_{\beta}^{x,y,z}\left[\kappa^{\omega}_{\alpha}, \left[\kappa^{-\omega}_{\beta}, \left[\kappa^{\omega}_{\beta}, F\right] + 3F^{\omega}_{\beta}\right] + \left[\kappa^{\omega}_{\beta}, \left[\kappa^{-\omega}_{\beta}, F\right] + 3F^{-\omega}_{\beta}\right] + 3F^{\omega,-\omega}_{\beta,\beta} + F^{-\omega,\omega}_{\beta,\beta}\right]. \quad (60)$$

We can combine all the terms as

$$\tau^{\alpha\alpha\beta\beta} + \tau^{\alpha\beta\alpha\beta} + \tau^{\alpha\beta\beta\alpha} = \Bigg[\kappa_\alpha^{\omega}, \sum_{\beta}^{x,y,z}\Big(\big[\kappa_\beta^{-\omega}, \big[\kappa_\beta^{\omega}, F\big] + 3F_\beta^{\omega}\big] + \big[\kappa_\beta^{\omega}, \big[\kappa_\beta^{-\omega}, F\big] + 3F_\beta^{-\omega}\big] + 3F_{\beta,\beta}^{-\omega,\omega} + 3F_{\beta,\beta}^{\omega,-\omega}\Big)$$
$$+ 2\big[\kappa_\alpha^{-\omega}, \big[\kappa_\alpha^{\omega}, F\big] + 3F_\beta^{\omega}\big] + 2\big[\kappa_\alpha^{\omega}, \big[\kappa_\alpha^{-\omega}, F\big] + 3F_\alpha^{-\omega}\big] + 6F_{\alpha,\alpha}^{-\omega,\omega} + 6F_{\alpha,\alpha}^{\omega,-\omega}\Bigg]$$
$$+ \sum_{\beta\neq\alpha}^{x,y,z}\Big(\big[\kappa_\beta^{\omega}, \big[\kappa_\alpha^{-\omega}, \big[\kappa_\beta^{\omega}, F\big] + 3F_\beta^{\omega}\big] + \big[\kappa_\beta^{\omega}, \big[\kappa_\alpha^{-\omega}, F\big] + 3F_\alpha^{-\omega}\big] + 3F_{\alpha,\beta}^{-\omega,\omega} + 3F_{\beta,\alpha}^{\omega,-\omega}$$
$$+ \big[\kappa_\beta^{-\omega}, \big[\kappa_\alpha^{\omega}, F\big] + 3F_\alpha^{\omega}\big] + \big[\kappa_\alpha^{\omega}, \big[\kappa_\beta^{-\omega}, F\big] + 3F_\beta^{-\omega}\big] + 3F_{\beta,\alpha}^{-\omega,\omega} + 3F_{\alpha,\beta}^{\omega,-\omega}\big]\Big)$$
$$= \sum_{\beta}^{x,y,z}\big[\kappa_\beta^{\omega}, \Theta_{\alpha\beta}^{\tau} + F_{\alpha\beta}^{\tau}\big], \tag{61}$$

where we have introduced the auxiliary matrices

$$\Theta_{\alpha\beta}^{\tau} = \big[\kappa_\alpha^{-\omega}, \big[\kappa_\beta^{\omega}, F\big] + 3F_\beta^{\omega}\big] + \big[\kappa_\beta^{\omega}, \big[\kappa_\alpha^{-\omega}, F\big] + 3F_\alpha^{-\omega}\big]$$
$$+ \big[\kappa_\beta^{-\omega}, \big[\kappa_\alpha^{\omega}, F\big] + 3F_\alpha^{\omega}\big] + \big[\kappa_\alpha^{\omega}, \big[\kappa_\beta^{-\omega}, F\big] + 3F_\beta^{-\omega}\big]$$
$$+ \delta_{\alpha\beta}\sum_{\rho}^{x,y,z}\Big(\big[\kappa_\rho^{\omega}, \big[\kappa_\rho^{-\omega}, F\big] + 3F_\rho^{-\omega}\big] + \big[\kappa_\rho^{-\omega}, \big[\kappa_\rho^{\omega}, F\big] + 3F_\rho^{\omega}\big]\Big), \tag{62}$$

$$F_{\alpha\beta}^{\tau} = 3\big(F_{\alpha,\beta}^{-\omega,\omega} + F_{\beta,\alpha}^{\omega,-\omega} + F_{\beta,\alpha}^{-\omega,\omega} + F_{\alpha,\beta}^{\omega,-\omega}\big)$$
$$+ 3\delta_{\alpha\beta}\sum_{\rho}^{x,y,z}\big(F_{\rho,\rho}^{-\omega,\omega} + F_{\rho,\rho}^{\omega,-\omega}\big). \tag{63}$$

The first index in $F_{\alpha\beta}^{\tau}$ refers to that the first index in the gamma tensors whose τ components were added was set to α and the second index refers to that the fourth operator in the added gamma tensors was set to β since the leading terms of all τ terms get their components from the fourth operator of the gamma tensor [see Eq. (22)], while the second and third operators run through all possible values such that the combination of operators still belongs to the set of gamma tensors that exist in the isotropic average.

From Eqs. (50) and (61), we see that we can add the terms involving λ and τ since the they have the same matrix in the leading term, which results in a newly defined two-time transformed compounded first-order Fock matrix,

$$F_{\alpha\beta}^{(\lambda+\tau)} = 6F_{\alpha,\beta}^{-\omega,\omega} + 6F_{\beta,\alpha}^{-\omega,\omega} + 6F_{\beta,\alpha}^{-\omega,\omega} + 6F_{\alpha,\beta}^{\omega,-\omega}$$
$$+ \delta_{\alpha,\beta}\sum_{\rho}^{x,y,z}\big(6F_{\rho,\rho}^{-\omega,\omega} + 6F_{\rho,\rho}^{\omega,-\omega}\big). \tag{64}$$

For the three-time transformed first-order compounded Fock matrices, we get from $\gamma_{\alpha\alpha\beta\beta}$, $\gamma_{\alpha\beta\beta\alpha}$, and $\gamma_{\alpha\beta\alpha\beta}$ that

$$F_\alpha^{\lambda\sigma\tau} = F^{(\beta\alpha\beta)} + F^{(\beta\beta\alpha)} + F^{(\beta\alpha\alpha)}, \tag{65}$$

where

$$F^{(\alpha\beta\beta)} = \sum_{\beta}^{x,y,z}\big(F_{\alpha\beta\beta}^{\omega,-\omega,\omega} + F_{\alpha\beta\beta}^{\omega,\omega,-\omega} + F_{\beta\alpha\beta}^{-\omega,\omega,\omega} + F_{\beta\beta\alpha}^{-\omega,\omega,\omega}$$
$$+ F_{\beta\beta\alpha}^{\omega,-\omega,\omega} + F_{\beta\alpha\beta}^{\omega,\omega,-\omega}\big), \tag{66}$$

$$F^{(\beta\beta\alpha)} = \sum_{\beta}^{x,y,z}\big(F_{\beta\beta\alpha}^{\omega,-\omega,\omega} + F_{\beta\alpha\beta}^{\omega,\omega,-\omega} + F_{\beta\beta\alpha}^{-\omega,\omega,\omega} + F_{\beta\alpha\beta}^{-\omega,\omega,\omega}$$
$$+ F_{\alpha\beta\beta}^{\omega,-\omega,\omega} + F_{\alpha\beta\beta}^{\omega,\omega,-\omega}\big), \tag{67}$$

$$F^{(\beta\alpha\beta)} = \sum_{\beta}^{x,y,z}\big(F_{\beta\alpha\beta}^{\omega,-\omega,\omega} + F_{\beta\beta\alpha}^{\omega,\omega,-\omega} + F_{\alpha\beta\beta}^{-\omega,\omega,\omega} + F_{\alpha\beta\beta}^{-\omega,\omega,\omega}$$
$$+ F_{\beta\alpha\beta}^{\omega,-\omega,\omega} + F_{\beta\beta\alpha}^{\omega,\omega,-\omega}\big). \tag{68}$$

Finally, we can combine Eqs. (64), (57), and (65) to get the total perturbed Fock matrix as

$$\overline{\overline{F}}_\alpha = \sum_{\beta}^{x,y,z}\Big(\big[\kappa_\beta^{\omega}, \Theta_{\alpha\beta}^{(\lambda+\tau)} + F_{\alpha\beta}^{(\lambda+\tau)}\big] + \big[\kappa_\beta^{-\omega}, \Theta_{\alpha\beta}^{\sigma} + F_{\alpha\beta}^{\sigma}\big]\Big) + F_\alpha^{\lambda\sigma\tau}. \tag{69}$$

Thus, the total $E^{[4]}$ contraction of Eq. (46) can be written with Eq. (69) as

$$\sum_{\alpha,\beta}^{x,y,z} N_{j;\alpha}^{-\omega} E_{j(klm)}^{[4]}\big[N_{k;\alpha}^{\omega} N_{l;\beta}^{-\omega} N_{m;\beta}^{\omega} + N_{k;\beta}^{\omega} N_{l;\alpha}^{-\omega} N_{m;\beta}^{\omega} + N_{k;\beta}^{\omega} N_{l;\beta}^{-\omega} N_{m;\alpha}^{\omega}\big]$$
$$= -2\sum_{\alpha,\beta}^{x,y,z} N_{j;\alpha}^{-\omega}\begin{bmatrix}\Big(\big[\kappa_\beta^{\omega}, \Theta_{\alpha\beta}^{(\lambda+\tau)} + F_{\alpha\beta}^{(\lambda+\tau)}\big] + \big[\kappa_\beta^{-\omega}, \Theta_{\alpha\beta}^{\sigma} + F_{\alpha\beta}^{\sigma}\big] + F_\alpha^{\lambda\sigma\tau}\Big)_{is}\\ -\Big(\big[\kappa_\beta^{\omega}, \Theta_{\alpha\beta}^{(\lambda+\tau)} + F_{\alpha\beta}^{(\lambda+\tau)}\big] + \big[\kappa_\beta^{-\omega}, \Theta_{\alpha\beta}^{\sigma} + F_{\alpha\beta}^{\sigma}\big] + F_\alpha^{\lambda\sigma\tau}\Big)_{si}\end{bmatrix}. \tag{70}$$

The number of Fock matrices needed to evaluate Eq. (70) can be reduced further by realizing symmetries within the compounded Fock matrices. From the definition of $F^{(\lambda+\tau)}_{\alpha\beta}$ and $F^{\sigma}_{\alpha\beta}$, we see that if we reverse the indices, the compounded Fock matrix is unchanged, provided that $\alpha \neq \beta$,

$$F^{\sigma}_{\beta\alpha} = F^{\sigma}_{\alpha\beta}, \quad F^{(\lambda+\tau)}_{\beta\alpha} = F^{(\lambda+\tau)}_{\alpha\beta}, \quad \alpha \neq \beta. \tag{71}$$

Next, we consider the densities required for the computation of the compounded Fock matrices. From Eq. (64), we get

$$D^{(\lambda+\tau)}_{\alpha\beta} = 6\left[\kappa^{-\omega}_{\alpha}, D^{\omega}_{\beta}\right] + 6\left[\kappa^{-\omega}_{\beta}, D^{\omega}_{\alpha}\right] + 6\left[\kappa^{\omega}_{\alpha}, D^{-\omega}_{\beta}\right] + 6\left[\kappa^{\omega}_{\beta}, D^{-\omega}_{\alpha}\right] + 6\delta_{\alpha\beta}\sum_{\rho}^{x,y,z}\left(\left[\kappa^{-\omega}_{\rho}, D^{\omega}_{\rho}\right] + \left[\kappa^{\omega}_{\rho}, D^{-\omega}_{\rho}\right]\right). \tag{72}$$

Likewise from Eq. (57), we obtain

$$D^{\sigma}_{\alpha\beta} = 6\left[\kappa^{\omega}_{\alpha}, D^{\omega}_{\beta}\right] + 6\left[\kappa^{\omega}_{\beta}, D^{\omega}_{\alpha}\right] + 6\delta_{\alpha\beta}\sum_{\rho}^{x,y,z}\left(\left[\kappa^{\omega}_{\rho}, D^{\omega}_{\rho}\right]\right). \tag{73}$$

Using Eqs. (66)–(68), we can write the compounded densities for the three-indexed first-order densities in terms of the two-time transformed first-order densities as

$$D^{(\alpha\beta\beta)} = \sum_{\beta}^{x,y,z}\left(\left[\kappa^{\omega}_{\alpha}, D^{-\omega,\omega}_{\beta\beta} + D^{\omega,-\omega}_{\beta\beta}\right] + \left[\kappa^{-\omega}_{\beta}, D^{\omega,\omega}_{\alpha\beta} + D^{\omega,\omega}_{\beta\alpha}\right] + \left[\kappa^{\omega}_{\beta}, D^{-\omega,\omega}_{\beta\alpha} + D^{\omega,-\omega}_{\alpha\beta}\right]\right), \tag{74}$$

$$D^{(\beta\beta\alpha)} = \sum_{\beta}^{x,y,z}\left(\left[\kappa^{\omega}_{\beta}, D^{-\omega,\omega}_{\beta\alpha} + D^{\omega,-\omega}_{\alpha\beta}\right] + \left[\kappa^{-\omega}_{\beta}, D^{\omega,\omega}_{\beta\alpha} + D^{\omega,\omega}_{\alpha\beta}\right] + \left[\kappa^{\omega}_{\alpha}, D^{-\omega,\omega}_{\beta\beta} + D^{\omega,-\omega}_{\beta\beta}\right]\right), \tag{75}$$

$$D^{(\beta\alpha\beta)} = \sum_{\beta}^{x,y,z}\left(\left[\kappa^{\omega}_{\beta}, D^{-\omega,\omega}_{\alpha\beta} + D^{\omega,-\omega}_{\beta\alpha}\right] + \left[\kappa^{-\omega}_{\alpha}, D^{\omega,\omega}_{\beta\beta} + D^{\omega,\omega}_{\beta\beta}\right] + \left[\kappa^{\omega}_{\beta}, D^{-\omega,\omega}_{\alpha\beta} + D^{\omega,-\omega}_{\beta\alpha}\right]\right). \tag{76}$$

The three-time transformed first-order densities can be written in terms of the compounded two-time transformed densities as

$$D^{(\alpha\beta\beta)} + D^{(\beta\beta\alpha)} + D^{(\beta\alpha\beta)} = \sum_{\beta}^{x,y,z}\left[\kappa^{-\omega}_{\beta}, \frac{1}{3}D^{\sigma}_{\alpha\beta}\right] + \left[\kappa^{\omega}_{\beta}, \frac{1}{3}D^{\lambda+\tau}_{\alpha\beta}\right]. \tag{77}$$

Using density addition, one can also rewrite the $E^{[3]}$ contractions in terms of compounded Fock matrices. The Fock matrices within the commutators of the contraction of the $E^{[3]}$ tensor can be extracted from the subspace of the response solver; thus, the explicit goal of this section is not to minimize the number of Fock matrices within the commutators; instead, the optimization goal is to add as many compounded second-order response vectors and minimize the number of Fock matrices outside the commutators with density addition. There are some constraints to which second-order response vectors can be added. The first constraint is, as can be seen from Eqs. (43) and (44), that the frequency arguments of the response vectors that are to be added must be the same in order to be able to solve a compounded response vector from the response equations by a single matrix inversion. The second constraint is that once compounded response vectors are obtained, one can no longer obtain all the individual Fock matrices. Thus, one can only add the response vectors that correspond to the Fock matrices that are within the commutators that can also be added using density addition [see Eq. (45)]. Furthermore, one additional constraint is that the compounded second-order response vectors must be defined in a manner in which the property gradients used to form them can be written in terms of the compounded Fock matrices [see Eqs. (57) and (64)]. Since the second-order response vectors possess permutation symmetry with respect to the interchange of operator and frequency pairs [see Eq. (30)], we can use Eqs. (40), (14), and (25) to write the total contraction of the $E^{[3]}$ tensors as

$$\sum_{\alpha,\beta}^{x,y,z} N^{-\omega}_{j;\alpha} E^{[3]}_{j(kl)}\left(2N^{\omega}_{k;\beta}\left(N^{-\omega,\omega}_{l;\beta,\alpha} + N^{-\omega,\omega}_{l;\alpha,\beta}\right) + 2N^{\omega}_{k;\alpha}N^{-\omega,\omega}_{l;\beta,\beta} + N^{-\omega}_{k;\alpha}N^{\omega,\omega}_{l;\beta,\beta} + N^{-\omega}_{k;\beta}\left(N^{\omega,\omega}_{l;\alpha,\beta} + N^{\omega,\omega}_{l;\beta,\alpha}\right)\right)$$
$$= -2\sum_{\alpha,\beta}^{x,y,z} N^{-\omega}_{j;\alpha}\begin{bmatrix}\left(2\zeta^{\omega,(-\omega,\omega)}_{\beta,\beta\alpha} + 2\zeta^{\omega,(-\omega,\omega)}_{\beta,\alpha\beta} + 2\zeta^{\omega,(-\omega,\omega)}_{\alpha,\beta\beta} + \zeta^{\omega,(\omega,\omega)}_{\alpha,\beta\beta} + \zeta^{\omega,(\omega,\omega)}_{\beta,\alpha\beta} + \zeta^{\omega,(\omega,\omega)}_{\beta,\beta\alpha} + F^{\lambda,\sigma\tau}_{\alpha}\right)_{si} \\ \left(2\zeta^{\omega,(-\omega,\omega)}_{\beta,\beta\alpha} + 2\zeta^{\omega,(-\omega,\omega)}_{\beta,\alpha\beta} + 2\zeta^{\omega,(-\omega,\omega)}_{\alpha,\beta\beta} + \zeta^{\omega,(\omega,\omega)}_{\alpha,\beta\beta} + \zeta^{\omega,(\omega,\omega)}_{\beta,\alpha\beta} + \zeta^{\omega,(\omega,\omega)}_{\beta,\beta\alpha} + F^{\lambda,\sigma\tau}_{\alpha}\right)_{is}\end{bmatrix}. \tag{78}$$

We now proceed to define the second-order response vectors that can be added using gradient addition. We first apply the frequency constraint on the response vectors [see Eqs. (79) and (81)] we wish to combine. We thus start with the first term in the first sum of Eq. (78), and we divide this term into two sums as dictated by the density addition constraint [Eq. (45)], which dictates that the first-order response vectors must be the same such that we may add the Fock matrices within the commutators,

$$\sum_{\beta}^{x,y,z}\left[2N^{\omega}_{k;\beta}\left(N^{-\omega,\omega}_{l;\beta,\alpha} + N^{-\omega,\omega}_{l;\alpha,\beta}\right) + 2N^{\omega}_{k;\alpha}N^{-\omega,\omega}_{l;\beta,\beta}\right]$$
$$= \sum_{\beta\neq\alpha}^{x,y,z} 2N^{\omega}_{k;\beta}\left(N^{-\omega,\omega}_{l;\beta,\alpha} + N^{-\omega,\omega}_{l;\alpha,\beta}\right) + 4N^{\omega}_{k;\alpha}N^{-\omega,\omega}_{l;\alpha,\alpha} + 2\sum_{\beta}^{x,y,z} N^{\omega}_{k;\alpha}N^{-\omega,\omega}_{l;\beta,\beta}. \tag{79}$$

We can see that if we introduce the Kronecker delta function and the dummy variable ρ, we can rewrite Eq. (79) and implicitly define one set of compounded second-order response vectors as

$$\sum_{\beta}^{x,y,z} N_{k;\beta}^{\omega}\left[2\left(N_{l;\beta,\alpha}^{-\omega,\omega}+N_{l;\alpha,\beta}^{-\omega,\omega}\right)+2\delta_{\alpha\beta}\sum_{\rho}^{x,y,z}N_{l;\rho\rho}^{-\omega,\omega}\right] \equiv \sum_{\beta}^{x,y,z} N_{k;\beta}^{\omega}N_{l;\alpha,\beta}^{(\lambda+\tau)}. \tag{80}$$

In the same way, we can implicitly define a second set of compounded response vectors from the second term in the first sum of Eq. (78) as

$$\begin{aligned}\sum_{\beta}^{x,y,z}&\left[N_{k;\alpha}^{-\omega}N_{l;\beta,\beta}^{\omega,\omega}+N_{k;\beta}^{-\omega}\left(N_{l;\alpha,\beta}^{\omega,\omega}+N_{l;\beta,\alpha}^{\omega,\omega}\right)\right]\\ &=\sum_{\beta\neq\alpha}^{x,y,z}2N_{k;\beta}^{-\omega}N_{l;\beta,\alpha}^{\omega,\omega}+2N_{k;\alpha}^{-\omega}N_{l;\alpha,\alpha}^{\omega,\omega}+\sum_{\beta}^{x,y,z}N_{k;\alpha}^{-\omega}N_{l;\beta,\beta}^{\omega,\omega}\\ &=\sum_{\beta}^{x,y,z}N_{k;\beta}^{-\omega}\left[2N_{l;\alpha,\beta}^{\omega,\omega}+\delta_{\alpha\beta}\sum_{\rho}^{x,y,z}N_{l;\rho,\rho}^{-\omega,\omega}\right]\equiv\sum_{\beta}^{x,y,z}N_{k;\beta}^{-\omega}N_{l;\alpha,\beta}^{\sigma}.\end{aligned} \tag{81}$$

The explicit expressions for these compounded second-order response vectors become

$$N_{j;\alpha,\beta}^{(\lambda+\tau)}=2N_{j;\alpha,\beta}^{-\omega,\omega}+2N_{j;\beta,\alpha}^{-\omega,\omega}+\delta_{\alpha\beta}\sum_{\rho}^{x,y,z}2N_{j;\rho,\rho}^{-\omega,\omega}, \tag{82}$$

$$N_{j;\alpha,\beta}^{\sigma}=2N_{j;\alpha,\beta}^{\omega,\omega}+\delta_{\alpha\beta}\sum_{\rho}^{x,y,z}N_{j;\rho,\rho}^{\omega,\omega}. \tag{83}$$

From Eqs. (82) and (83), we see that the compounded response vectors also possess permutation symmetry in the interchange of α and β when $\beta\neq\alpha$,

$$N_{\alpha,\beta}^{(\lambda+\tau)}=N_{\beta,\alpha}^{(\lambda+\tau)},\quad N_{\alpha,\beta}^{\sigma}=N_{\beta,\alpha}^{\sigma}\quad \alpha\neq\beta. \tag{84}$$

The fact that there are repetitions of elements such as γ_{xxxx} in $\bar{\gamma}$ gives rise to the α-dependent additional terms $4N_{l;\alpha,\alpha}^{\omega,-\omega}$ and $2N_{l;\alpha,\alpha}^{\omega,\omega}$ that break the symmetry when $\beta=\alpha$. There will thus be six unique compounded response vectors for each frequency for $N_{l;\alpha\beta}^{\sigma\sigma}$ and $N_{l;\alpha\beta}^{(\lambda\lambda+\tau\tau)}$, respectively. In order for these compounded response vectors to be usable, one also needs to be able to express their compounded property gradients in terms of the compounded Fock matrices otherwise, one would need to compute new Fock matrices that would render the whole method inefficient. The compounded response vectors are solutions to equations of the form

$$N_{\alpha,\beta}^{(\lambda+\tau)}=(E^{[2]}-i\gamma R^{[2]})^{-1}\Lambda_{\alpha,\beta}^{(\lambda+\tau)}, \tag{85}$$

$$N_{\alpha,\beta}^{\sigma}=(E^{[2]}-2\omega S^{[2]}+i\gamma R^{[2]})^{-1}\Lambda_{\alpha,\beta}^{\sigma}. \tag{86}$$

The property gradients are obtained by combining the expression for the second-order property gradient [Eq. (11)] with the expression for the second-order response vectors [Eq. (9)] together with newly defined compounded second-order response vectors defined in Eqs. (82) and (83). As the gradient for Eq. (86), we obtain

$$\begin{aligned}\Lambda_{j;\alpha,\beta}^{\sigma}&=2\Lambda_{j;\alpha,\beta}^{\omega,\omega}+\delta_{\alpha,\beta}\sum_{\rho}^{x,y,z}\Lambda_{j;\rho,\rho}^{\omega,\omega}\\ &=2\mu_{jk;\alpha}^{[2]}N_{k;\beta}^{\omega}+2\mu_{jk;\beta}^{[2]}N_{k;\alpha}^{\omega}-2E_{j(kl)}^{[3]}N_{k;\alpha}^{\omega}N_{l;\beta}^{\omega}\\ &\quad+\delta_{\alpha\beta}\sum_{\rho}^{x,y,z}\left(2\mu_{jk;\rho}^{[2]}N_{k;\rho}^{\omega}-E_{j(kl)}^{[3]}N_{k;\rho}^{\omega}N_{l;\rho}^{\omega}\right),\end{aligned} \tag{87}$$

which can be rewritten in terms of one- and two-time transformed first-order Fock matrices by applying Eqs. (15)–(18) to two first-order response vectors,

$$\begin{aligned}\Lambda_{j;\alpha,\beta}^{\sigma}&=2\mu_{jk;\beta}^{[2]}N_{k;\alpha}^{\omega}+2\mu_{jk;\alpha}^{[2]}N_{k;\beta}^{\omega}-2\zeta_{j;\alpha,\beta}^{\omega,\omega}-2F_{j;\alpha,\beta}^{\omega,\omega}-2F_{j;\beta,\alpha}^{\omega,\omega}\\ &\quad+\sum_{\rho}^{x,y,z}\left(2\mu_{jk;\rho}^{[2]}N_{k;\rho}^{\omega}-\zeta_{j;\rho\rho}^{\omega,\omega}-2F_{j;\rho\rho}^{\omega,\omega}\right).\end{aligned} \tag{88}$$

We can now verify that the compounded gradients can indeed be written in terms of the compounded Fock matrices of Eqs. (57) and (64) as

$$\begin{aligned}\Lambda_{j;\alpha,\beta}^{\sigma}&=2\mu_{jk;\beta}^{[2]}N_{k;\alpha}^{\omega}+2\mu_{jk;\alpha}^{[2]}N_{k;\beta}^{\omega}-2\zeta_{j;\alpha,\beta}^{\omega,\omega}-\frac{1}{3}F_{j;\alpha,\beta}^{\sigma}\\ &\quad+\delta_{\alpha\beta}\sum_{\rho}^{x,y,z}\left(2\mu_{jk;\rho}^{[2]}N_{k;\rho}^{\omega}-\zeta_{j;\rho,\rho}^{\omega,\rho}\right).\end{aligned} \tag{89}$$

Likewise, for the gradients of Eq. (85), we obtain

$$\begin{aligned}\Lambda_{j;\alpha,\beta}^{(\lambda+\tau)}&=2\Lambda_{j;\alpha,\beta}^{-\omega,\omega}+2\Lambda_{j;\beta,\alpha}^{-\omega,\omega}+\delta_{\alpha\beta}\sum_{\rho}^{x,y,z}2\Lambda_{j;\rho,\rho}^{-\omega,\omega}\\ &=2\mu_{jk;\beta}^{[2]}\left[N_{k;\alpha}^{-\omega}+N_{k;\alpha}^{\omega}\right]+2\mu_{jk;\alpha}^{[2]}\left[N_{k;\beta}^{-\omega}+N_{k;\beta}^{\omega}\right]\\ &\quad-2E_{j(kl)}^{[3]}N_{k;\alpha}^{-\omega}N_{l;\beta}^{\omega}-2E_{j(kl)}^{[3]}N_{k;\alpha}^{\omega}N_{l;\beta}^{-\omega}\\ &\quad+\delta_{\alpha\beta}\sum_{\rho}^{x,y,z}\left(2\mu_{jk;\rho}^{[2]}\left[N_{k;\rho}^{-\omega}+N_{k;\rho}^{\omega}\right]-2E_{j(kl)}^{[3]}N_{k;\rho}^{-\omega}N_{l;\rho}^{\omega}\right).\end{aligned} \tag{90}$$

Using Eqs. (15)–(18), Eq. (90) can be rewritten in terms of one- and two-time transformed Fock matrices as

$$\begin{aligned}\Lambda_{j;\alpha,\beta}^{(\lambda+\tau)}&=2\mu_{\beta}^{[2]}\left[N_{\alpha}^{-\omega}+N_{\alpha}^{\omega}\right]+2\mu_{\alpha}^{[2]}\left[N_{\beta}^{-\omega}+N_{\beta}^{\omega}\right]\\ &\quad-2\zeta_{\alpha\beta}^{-\omega,\omega}-2\zeta_{\beta\alpha}^{-\omega,\omega}-2F_{\alpha\beta}^{-\omega,\omega}-2F_{\beta\alpha}^{-\omega,\omega}\\ &\quad+\delta_{\alpha\beta}\sum_{\rho}^{x,y,z}\left(2\mu_{\rho}^{[2]}\left[N_{\rho}^{-\omega}+N_{\rho}^{\omega}\right]-2\zeta_{\rho\rho}^{-\omega,\omega}-2F_{\rho\rho}^{-\omega,\omega}-2F_{\rho\rho}^{\omega,-\omega}\right).\end{aligned} \tag{91}$$

We can now verify that the compounded gradients can be written in terms of the compounded Fock matrices (57) and (64) as

$$\begin{aligned}\Lambda_{j;\alpha,\beta}^{(\lambda+\tau)}&=2\mu_{\beta}^{[2]}\left[N_{\alpha}^{-\omega}+N_{\alpha}^{\omega}\right]+2\mu_{\alpha}^{[2]}\left[N_{\beta}^{-\omega}+N_{\beta}^{\omega}\right]-2\zeta_{\alpha\beta}^{-\omega,\omega}-2\zeta_{\beta\alpha}^{-\omega,\omega}\\ &\quad-\frac{1}{3}F_{\alpha\beta}^{(\lambda+\tau)}+\delta_{\alpha\beta}\sum_{\rho}^{x,y,z}\left(2\mu_{\rho}^{[2]}\left[N_{\rho}^{-\omega}+N_{\rho}^{\omega}\right]-2\zeta_{\rho\rho}^{-\omega,\omega}\right).\end{aligned} \tag{92}$$

The compounded gradients share the same symmetry as the compounded Fock matrices of Eqs. (57) and (64). We have thus derived compounded response vectors that abide to all three constraints and can now rewrite the expression for the total contraction of the $E^{[3]}$ tensor in Eq. (78) in terms of the compounded response vectors in Eqs. (82) and (83) as

$$\sum_{\alpha,\beta}^{x,y,z} N_{j;\alpha}^{-\omega} E_{j(kl)}^{[3]} \left(N_{k;\beta}^{\omega} N_{l;\alpha,\beta}^{(\lambda+\tau)} + N_{k;\beta}^{-\omega} N_{l;\alpha,\beta}^{\sigma} \right) = -2 \sum_{\alpha}^{x,y,z} N_{j;\alpha}^{-\omega} \left[\begin{pmatrix} \zeta_{\alpha}^{\sigma} + \zeta_{\alpha}^{(\lambda+\tau)} + F_{\alpha}^{\lambda\sigma,\tau} \end{pmatrix}_{si} \right]. \tag{93}$$

We here define the compounded vector elements using Eqs. (16)–(18) and (93) as

$$\zeta_{\alpha}^{\sigma} = \sum_{\beta}^{x,y,z} \left[\kappa_{\beta}^{-\omega}, \left[\kappa_{\alpha,\beta}^{\sigma}, F^0 \right] + 2F_{\alpha\beta}^{\sigma\sigma} \right] + \left[\kappa_{\alpha,\beta}^{\sigma}, \left[\kappa_{\beta}^{-\omega}, F^0 \right] + 2F_{\beta}^{-\omega} \right], \tag{94}$$

$$\zeta_{\alpha}^{(\lambda+\tau)} = \sum_{\beta}^{x,y,z} \left[\kappa_{\beta}^{\omega}, \left[\kappa_{\alpha,\beta}^{(\lambda+\tau)}, F^0 \right] + 2F_{\alpha\beta}^{(\lambda\lambda+\tau\tau)} \right] + \left[\kappa_{\alpha,\beta}^{(\lambda+\tau)}, \left[\kappa_{\beta}^{\omega}, F^0 \right] + 2F_{\beta}^{\omega} \right], \tag{95}$$

where the one-time transformed second-order compounded Fock matrices in Eqs. (94) and (95) are defined as

$$F_{\alpha\beta}^{\sigma\sigma} = D_{\alpha\beta}^{\sigma\sigma} \mathcal{L}, \tag{96}$$

$$F_{\alpha\beta}^{(\lambda\lambda+\tau\tau)} = D_{\alpha\beta}^{(\lambda\lambda+\tau\tau)} \mathcal{L}. \tag{97}$$

These compounded Fock matrices can be constructed as linear combinations of Fock matrices from the subspace of the iterative solver and the SCF Fock matrix as

$$\begin{bmatrix} (F_{\alpha\beta}^{\sigma\sigma})_{si} \\ -(F_{\alpha\beta}^{\sigma\sigma})_{is} \end{bmatrix} = E^{[2]} N_{\alpha,\beta}^{\sigma} - \begin{bmatrix} [\kappa_{\alpha,\beta}^{\sigma}, F^0]_{si} \\ -[\kappa_{\alpha,\beta}^{\sigma}, F^0]_{is} \end{bmatrix},$$
$$\begin{bmatrix} \left(F_{\alpha\beta}^{(\lambda\lambda+\tau\tau)}\right)_{si} \\ -\left(F_{\alpha\beta}^{(\lambda\lambda+\tau\tau)}\right)_{is} \end{bmatrix} = E^{[2]} N_{\alpha,\beta}^{(\lambda+\tau)} - \begin{bmatrix} [\kappa_{\alpha,\beta}^{(\lambda+\tau)}, F^0]_{si} \\ -[\kappa_{\alpha,\beta}^{(\lambda+\tau)}, F^0]_{is} \end{bmatrix}. \tag{98}$$

However, the second-order two-time transformed Fock matrices must be determined as

$$F_{\alpha}^{\lambda,\sigma\tau} = D_{\alpha}^{\lambda,\sigma\tau} \mathcal{L}, \tag{99}$$

where the compounded densities are given by

$$D_{\alpha\beta}^{\sigma\sigma} = \left[\kappa_{\alpha\beta}^{\sigma}, D^0 \right], \tag{100}$$

$$D_{\alpha\beta}^{(\lambda\lambda+\tau\tau)} = \left[\kappa_{\alpha\beta}^{(\lambda+\tau)}, D^0 \right], \tag{101}$$

$$D_{\alpha}^{\lambda,\sigma\tau} = \sum_{\beta}^{x,y,z} \left(\left[\kappa_{\beta}^{-\omega}, D_{\alpha\beta}^{\sigma\sigma} \right] + \left[\kappa_{\alpha\beta}^{\sigma\sigma}, D_{\beta}^{-\omega} \right] + \left[\kappa_{\beta}^{\omega}, D_{\alpha\beta}^{(\lambda\lambda+\tau\tau)} \right] + \left[\kappa_{\alpha\beta}^{(\lambda\lambda+\tau\tau)}, D_{\beta}^{\omega} \right] \right). \tag{102}$$

5. One-photon off-resonance regions

All the Fock matrices defined up to this point obtain their frequency dependence from either the first-order response vectors [Eq. (8)] or the second-order response vectors [Eq. (9)] and thus exhibit different frequency dependent behaviors. Insights can be drawn from exact state response theory in order to further optimize the approximate state theory implementation. In exact response theory, the one-photon transition frequencies ω_k from state $|0\rangle$ to excited state $|k\rangle$ can be obtained by solving the generalized response eigenvalue equation. The response vectors in Eqs. (8), (85), and (86) in damped exact theory can be written in terms of the transition frequencies ω_k as

$$N_{k;\alpha}^{\omega} = \frac{\mu_{k;\alpha}}{\omega_{|k|} - \mathrm{sgn}(k)(\omega + i\gamma)}, \tag{103}$$

$$N_{k;\alpha,\beta}^{(\lambda+\tau)} = \frac{\Lambda_{k;\alpha,\beta}^{(\lambda+\tau)}}{\omega_{|k|} - i\mathrm{sgn}(k)\gamma}, \tag{104}$$

$$N_{k;\alpha,\beta}^{\sigma} = \frac{\Lambda_{k;\alpha,\beta}^{\sigma}}{\omega_{|k|} - \mathrm{sgn}(k)(2\omega + i\gamma)}. \tag{105}$$

The elements of the damped response vectors in Eq. (103) can be decomposed into real and imaginary parts, assuming that the gradient is real, and the components can be expressed as

$$(N_{k;\alpha}^{\omega})^{\mathcal{R}} = \frac{\mathrm{sgn}(k)(\omega_{|k|} - \mathrm{sgn}(k)\omega)\mu_{k;\alpha}}{(\omega_{|k|} - \mathrm{sgn}(k)\omega)^2 + \gamma^2},$$
$$(N_{k;\alpha}^{\omega})^{\mathcal{I}} = \frac{\mathrm{sgn}(k)\gamma\mu_{k;\alpha}}{(\omega_{|k|} - \mathrm{sgn}(k)\omega)^2 + \gamma^2}. \tag{106}$$

Equation (106) implies that when the optical frequency ω is far from any one-photon transition frequency ω_k, the imaginary part of the response vectors approaches zero much faster than the real part, and thus, the response vectors will be real for all practical purposes,

$$N_{\alpha}^{\omega} \approx (N_{\alpha}^{\omega})^{\mathcal{R}} \quad \text{for} \quad |\omega_k \pm \omega| \gg \gamma. \tag{107}$$

The second-order response vectors, however, display quite a different behavior. In the expression for the second-order hyperpolarizability, there are two fundamentally different types of second-order response vectors, as can be seen in Eqs. (104) and (105). The response vector from Eq. (105) will have non-zero imaginary elements as $2\omega \to \omega_k$, and they will thus have resonance at half the frequency of the single-indexed response vectors of Eq. (103). Furthermore, there are two fundamentally different types of two-photon excitations: those that are mediated through a virtual state $|0\rangle \to |v\rangle \to |f\rangle$ and those that pass through a real state $|0\rangle \to |m\rangle \to |f\rangle$. The latter occur if both $\omega_k/2$ and ω_k are eigenvalues of the generalized eigenvalue equation. The full cubic response equation can handle both these cases, but we can obtain significant reductions in the computational cost if we limit ourselves to the case when we pass through a virtual state before exciting to the final state. This case is very similar to the residual based method of obtaining second-order

transition amplitudes from the residual of the quadratic response function. In the regions far from resonances of Eq. (103), many of the first-order Fock matrices will have zero imaginary components. The fact that the first-order response vectors [Eq. (103)] are real in off-resonance regions implies that the first-order densities are real, and thus,

$$F_\alpha^\omega \approx (F_\alpha^\omega)^{\mathcal{R}} \quad \text{for} \quad |\omega_k \pm \omega| \gg \gamma. \tag{108}$$

Furthermore, since the two-time transformed first-order densities depend on the one-time transformed first-order densities, these likewise approach zero. As a result, the imaginary component of the two-time transformed first-order Fock matrices also approach zero, and since the compounded Fock matrices are formally sums of these Fock matrices, their imaginary components will also approach zero in optical regions far from any one-photon transition frequency ω_k,

$$\begin{aligned} F_{\alpha,\beta}^{\omega,\omega} &\approx \left(F_{\alpha,\beta}^{\omega,\omega}\right)^{\mathcal{R}} \to F_{\alpha,\beta}^{(\lambda+\tau)} \\ &\approx \left(F_{\alpha,\beta}^{(\lambda+\tau)}\right)^{\mathcal{R}}, F_{\alpha,\beta}^{\sigma} \approx \left(F_{\alpha,\beta}^{\sigma}\right)^{\mathcal{R}} \quad \text{for} \quad |\omega_k \pm \omega| \gg \gamma. \end{aligned} \tag{109}$$

As a consequence of this, the imaginary component of the first-order three-indexed densities will also approach zero. This implies that the imaginary component of the three-time transformed first-order Fock matrices also approach zero in optical regions far from any one-photon transition frequencies ω_k,

$$F_{\alpha,\beta,\gamma}^{\omega,\omega,\omega} \approx \left(F_{\alpha,\beta,\gamma}^{\omega,\omega,\omega}\right)^{\mathcal{R}} \to F_\alpha^{(\sigma\lambda\tau)} \approx \left(F_\alpha^{(\sigma\lambda\tau)}\right)^{\mathcal{R}} \quad \text{for} \quad |\omega_k \pm \omega| \gg \gamma. \tag{110}$$

This, in turn, also has consequences for the property gradients that also get their frequency dependence from the first-order response vectors, as seen from Eqs. (89) and (92). Thus, in regions far from any one photon resonance, we get that the imaginary components of the compounded property gradients will approach zero,

$$\Lambda_{\alpha,\beta}^{\sigma} \approx \left(\Lambda_{\alpha,\beta}^{\sigma}\right)^{\mathcal{R}}, \qquad \Lambda_{\alpha,\beta}^{(\lambda+\tau)} \approx \left(\Lambda_{\alpha,\beta}^{(\lambda+\tau)}\right)^{\mathcal{R}} \quad \text{for} \quad |\omega_k \pm \omega| \gg \gamma. \tag{111}$$

Since the first-order response vectors are real in regions far from any one-photon resonance, this means that many of the terms in the imaginary component of the second-order hyperpolarizability approach zero. Thus, we have that for all the terms in Eq. (14) that get their frequency dependence from the first-order response vectors, in regions where $|\omega_k \pm \omega| \gg \gamma$,

$$\mathrm{Im}\left(N_{j;\alpha}^{-\omega} T_{jklm}^{[4]} N_{k;\beta}^{\omega} N_{l;\gamma}^{-\omega} N_{m;\delta}^{\omega}\right) \approx 0, \tag{112}$$

$$\mathrm{Im}\left(N_{j;\alpha}^{-\omega} E_{j(kl)}^{[3]} N_{k;\delta}^{\omega} N_{l;\beta\gamma}^{\omega,-\omega}\right) \approx 0, \tag{113}$$

$$\begin{aligned} \mathrm{Im}\Big(&N_{j;\alpha}^{-\omega} \mu_{jkl;\beta}^{[3]} N_{k;\gamma}^{\omega} N_{l;\delta}^{\omega} + N_{j;\alpha}^{-\omega} \mu_{jkl;\gamma}^{[3]} N_{k;\beta}^{\omega} N_{l;\delta}^{\omega} \\ &+ N_{j;\alpha}^{-\omega} \mu_{jkl;\delta}^{[3]} N_{k;\beta}^{\omega} N_{l;\gamma}^{-\omega} - \mu_{(jlk);\alpha}^{[3]} N_{j;\beta}^{\omega} N_{k;\gamma}^{-\omega} N_{l;\delta}^{\omega}\Big) \approx 0. \end{aligned} \tag{114}$$

Therefore, we are left with a computationally much less demanding expression for the imaginary part of the isotropic second-order hyperpolarizability when sufficiently far away from any one-photon transition frequencies ω_k,

$$\begin{aligned} \tilde{\gamma}^{\mathcal{I}}(-\omega;\omega,-\omega,\omega) = \mathrm{Im}\Bigg(&\sum_{\alpha,\beta}^{x,y,z}\Big(N_{j;\alpha}^{-\omega} E_{j(kl)}^{[3]} N_{k;\beta}^{-\omega} N_{l;\alpha\beta}^{\sigma} \\ &- N_{j;\alpha}^{-\omega} \mu_{jk;\beta}^{[2]} N_{k;\alpha\beta}^{\sigma} - \mu_{(jk);\alpha}^{[2]} N_{j;\beta}^{-\omega} N_{k;\alpha\beta}^{\sigma}\Big)\Bigg). \end{aligned} \tag{115}$$

6. Minimal set of Fock matrices

In this section, a comparison is made between the number of Fock matrices and response vectors required for the isotropic cubic response function using the tensor average algorithm and the tensor component algorithm. The quantities in Table I are given on a per frequency basis and are irrespective of the molecular system and basis set employed. The computation of the response vectors also requires $E^{[2]}$ tensor contractions that can be written in terms of Fock matrices. However, the exact number of Fock matrices needed for this step is system, basis set, and frequency dependent. Different systems, basis sets, and the proximity of the optical frequency to resonances will require different numbers of trial vectors to reach the convergence threshold. The latter aspect is due to the fact that the preconditioner becomes close to singular near resonances and, as a consequence, the convergence efficiency in general reduces.[55] The total number of response vectors and the total number of Fock matrices are not involved in the subspace method for the response equations, depending on which γ-components are involved in the isotropic cubic response function. To make the comparison as general as possible, it is therefore the total number of response vectors that is compared between the different levels of optimization. In Table I, the tensor component column refers to the algorithms treated in Secs. II B 1 and II B 2, where for each frequency, 21 γ-tensor components are calculated explicitly and added to evaluate Eq. (6). Algorithm A refers to the computation of the isotropic second-order hyperpolarizability when only computing unique Fock matrices and response vectors; it serves as a reference. Algorithm B refers to the use of density addition and subspace extraction. The tensor average column refers to the method described in Sec. II B 3, where one can obtain greater computational efficiency by computing sums of $\gamma_{\alpha\beta\gamma\delta}$ instead of the individual components explicitly.

In the off-resonance regions, we can reduce the number of Fock matrices since in these regions, the imaginary parts of the first-order Fock matrices approach zero. Comparing columns 1 and 2 with 5 and 6 in Table I, we see that we get ~72% reduction in the number of Fock matrices using the reduced expression with Algorithm A. We can however obtain an even greater efficiency while maintaining the full accuracy and getting the γ-tensor components explicitly by using Algorithm B developed in this paper. This is seen by comparing the first two columns with columns 3 and 4, which are for the full second-order hyperpolarizability, where we see that we get ~75% reduction in the number of Fock matrices required. The first two columns represent the unique Fock matrices, while columns 3 and 4 get the one-time transformed first-order Fock matrices from the subspace of the response solver in addition to adding the permutations of Fock matrices, as outlined in Sec. II B 2, while still returning all the 21 unique γ-tensor components explicitly. If we

TABLE I. Number of Fock matrices and response vectors per frequency for the calculation of TPA cross sections with different algorithms. Algorithms A and B are described in Secs. II B 1 and II B 2, respectively. Algorithms B and C both make use of the subspace extraction technique described in Sec. II B 3.

	Tensor components[a]								Tensor average[b]			
	Full[c]				Reduced[d]				Full[c]		Reduced[d]	
	A		B		A		B		C		C	
	Re	Im	Re	Im	Re	Im	Re	Im	Re	Im	Re	Im
First-order												
F_{α}	6	6	0	0	6	6	0	0	0	0	0	0
$F^{\sigma}_{\alpha\beta}$	9	9	6	6	9	9	6	0	6	6	6	0
$F^{(\lambda+\tau)}_{\alpha\beta}$	18	18	9	9	0	0	0	0	6	6	0	0
$F^{\sigma\lambda\tau}_{\alpha}$	63	63	15	15	0	0	0	0	3	3	0	0
Second-order												
$F^{(\lambda\lambda+\tau\tau)}_{\alpha\beta}$	9	9	0	0	0	0	0	0	0	0	0	0
$F^{\sigma\sigma}_{\alpha\beta}$	6	6	0	0	6	6	0	0	0	0	0	0
$F^{\sigma\lambda,\tau}_{\alpha}$	72	72	15	15	30	30	15	15	3	3	3	3
Total	183	183	45	45	51	51	21	15	18	18	9	3
Response vectors												
N_{α}	3	3	3	3	3	3	3	0	3	3	3	0
$N^{\sigma}_{\alpha\beta}$	6	6	6	6	9	9	6	6	6	6	6	6
$N^{(\lambda+\tau)}_{\alpha\beta}$	9	9	9	9	0	0	0	0	6	6	0	0
Total	18	18	18	18	12	12	9	6	15	15	9	6

[a]Refers to the approach described in Secs. II B 1 and II B 2.
[b]Refers to the approach described in Sec. II B 4.
[c]Includes the full set of terms in the evaluation of the γ-tensor as expressed in Eq. (14).
[d]Includes a reduced set of terms in the evaluation of the γ-tensor as expressed in Eq. (115).

use the reduced expression with Algorithm B, we obtain a reduction in the number of Fock matrices by ~90%, as can be seen by comparing columns 1 and 2 with 7 and 8. A further reduction can be achieved when using the tensor average algorithm developed in this paper together with the subspace extraction. Comparing the first two columns with columns 9 and 10, corresponding to the full calculation, we see that the tensor average method in conjunction with the subspace extraction method yields ~90% reduction in the number of Fock matrices with no loss in accuracy. In the tensor average algorithm, the information about the individual γ-components is only found implicitly within the tensor average, which is indeed the relevant quantity for the two-photon absorption cross section. Using the reduced expression with further use of the tensor average algorithm in the off-resonance region yields a reduction in the number of Fock matrices required by ~97%, as can be seen by comparing columns 1 and 2 with columns 11 and 12. The addition of gradients in the novel tensor average scheme also allows for the computation of fewer second-order response vectors as they are not solved explicitly but rather summed together. This is most relevant for the full calculation as most of the benefits comes from adding the $N^{(\lambda+\tau)}$ response vectors. Comparing column one with nine, we see that we get ~17% reduction in the number of response vectors using the tensor average method. In the off-resonance regions, we get a reduction of ~37%, which is due to the complete omission of the $N^{(\lambda+\tau)}$ vectors.

III. EXAMPLE CALCULATIONS

A. Computational details

We adopt optimized structures of 2,5-dibromo-1,4-bis(2-(4-diphenylaminophenyl)vinyl)-benzene (BPVB) and alanine–tryptophan (Ala–Trp) as obtained at the B3LYP-D3/6-31(d,p) level of theory; see Fig. 1. All response calculations were performed at the HF level of theory and using the VeloxChem program.[56] In these property calculations, we made use of the def2-SVPD basis set, corresponding to 545 and 1314 contracted basis functions for Ala–Trp and BPVB, respectively. For the additional set of 22 molecules used for the validation calculations, all molecules were optimized using tight binding DFT,[58] and the response calculations were performed at the HF/def2-SVP level of theory. A damping parameter of γ = 120 meV was employed throughout the present work. In the

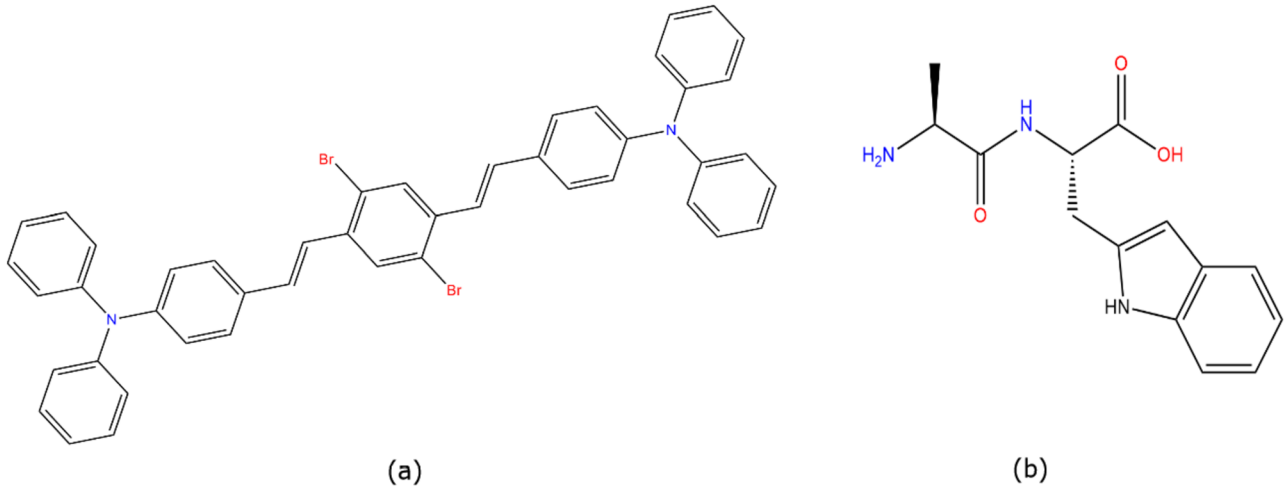

FIG. 1. Molecular structures of (a) BPVB and (b) Ala–Trp.

complex linear response equation solver, the relative convergence threshold was set to 10^{-3} with respect to the gradient norm.

B. 2,5-dibromo-1,4-bis (2-(4-diphenylaminophenyl)vinyl)-benzene

BPVB is a push–pull system with a large spin–orbit coupling that can act as an efficient triplet sensitizer,[59] and it is representative in size and has the π-conjugated character of two-photon active compounds used in real applications. The lowest band is found in the near UV region with a vertical transition energy of 3.47 eV. This theoretical estimate of the excitation energy is of course unrealistically high as our calculations are performed at the uncorrelated HF level of theory. So just to make it clear from the beginning, our goal in this section is not to make accurate predictions of any specific chromophore spectrum but merely to demonstrate the feasibility of treating systems of adequate size and excited-state character in the cubic response theory approach to TPA. The focus of the present work is to maximize the efficiency of the construction of Fock matrices, and choosing to illustrate our algorithms at the level of HF is relevant as the Coulomb and exchange contributions will be prevalent also at the level of DFT with the use of hybrid functionals.

In Fig. 2, the calculated TPA spectrum of BPVB is shown. The two approaches based on Eqs. (40) and (115) are denoted as "Full" and "Reduced," respectively. As shown in panel (a), the dominating TPA band in the low-energy region of the spectrum is found at a photon energy of 2.12 eV or likewise at an excitation energy of 4.24 eV. This result is a manifestation of the complementarity of one- and two-photon spectroscopies, where the former probes the electronic transition from the highest-occupied (HOMO) to the lowest unoccupied molecular orbital (LUMO) forming the S_1 state and the latter probes a higher-lying state, in this case state S_3, of a different symmetry character.

As shown in Fig. 2(a), the reduced expressions for the two-photon absorption cross section are quantitatively accurate with a relative error of less than 5% in the shown spectral region where the photon energy is detuned by at least 1.2 eV from the lowest one-photon resonance. In this off-resonance region, the dominating contributions to the TPA cross section stem from the $\mu^{[2]}$ terms as is seen by comparing the spectrum decomposition depicted in panels (b)–(d).

In Fig. 3, we shift focus to the one-photon resonance region. Here, there are important contributions also from the imaginary part of the first-order response vectors as illustrated by the presentation of the summed norm of the imaginary parts of these response vectors; see the green dashed curve in panel (a). In this resonance region, there are large negative contributions to $\sigma^{(2)}$ from all types of terms, as shown in panels (b)–(d). However, the physical total absorption cross section will remain positive as in this region it will be dominated by the positive $\sigma^{(1)}$-term in the expansion. Rather surprisingly, the $\sigma^{(2)}$ spectrum based on the reduced expression agrees well with that based on the full expression also in the one-photon resonance region. This is, however, a finding that is specific to this particular system and cannot be exploited in the general case.

C. Alanine–tryptophan

The Ala–Trp dipeptide has a high density of states in the UV region, and in such a situation, it can be advantageous to use the cubic-response rather than the quadratic-response residue based approach to calculate the TPA spectrum as the latter requires a spectral resolution. The 30 lowest excited singlet states of Ala-Try are presented in Fig. 4 with vertical bars representing the corresponding oscillator strengths. The lowest $S_1 \leftarrow S_0$ transition is found at 2.6 eV, which means that the first one-photon resonance in the TPA spectrum will occur at an excitation energy of 5.2 eV.

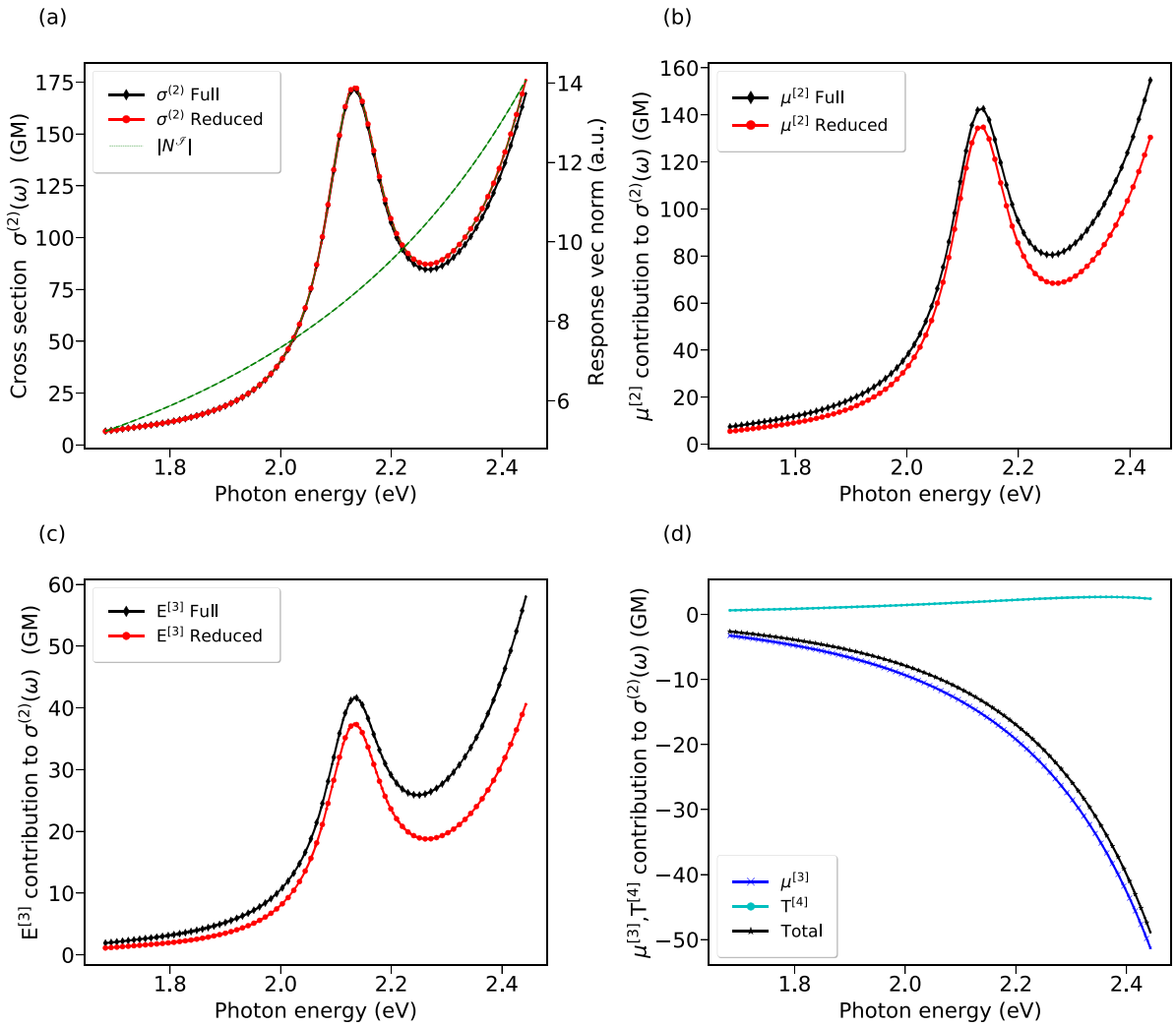

FIG. 2. Two-photon absorption spectra of BPVB in the off-resonance region at the HF/def2-SVPD level of theory: (a) total two-photon absorption cross section $\sigma^{(2)}$. The total magnitude of the imaginary component of the first-order response vectors $|N^{\mathcal{I}}| = \sum_{\alpha}^{x,y,z} |N_{\alpha}^{\mathcal{I}}|$; (b) contributions to $\sigma^{(2)}$ from $\mu^{[2]}$; (c) contributions to $\sigma^{(2)}$ from $E^{[3]}$; and (d) contributions to $\sigma^{(2)}$ from $T^{[4]}$ and $\mu^{[3]}$.

The TPA spectrum in Fig. 4 refers to the one-photon off-resonance region, and it is calculated based on the full [Eq. (14)] as well as the reduced [Eq. (115)] expressions for the isotropic second-order hyperpolarizability. The strongest TPA bands in this region are found between 4.0 eV and 4.3 eV, and they are thus associated with rather highly excited states in the spectrum. It can be clearly seen that the full and the reduced expressions for the TPA cross section give rise to nearly identical results. As one approaches the one-photon resonance at around 5.2 eV, the cross sections based on the reduced and full cubic response functions start to differ but only so slightly. This is further analyzed in Fig. 5, where we present the different types of contributions to the TPA cross section as well as the norm of the imaginary component of the first-order response vectors in panel (a). We note a near perfect agreement for $\sigma^{(2)}$-contributions from $\mu^{[2]}$ [panel (b)] and $E^{[3]}$ [panel (c)] terms and a fortuitous partial cancellation of the $\mu^{[3]}$ and $T^{[4]}$ terms [panel (d)] that are not included in the reduced expression.

As we get within 0.4 eV of the one-photon resonance, the imaginary part of the first-order response vectors becomes large, as shown in Fig. 6(a). The $T^{[4]}$ and $\mu^{[3]}$ contributions start to play a more prominent role. The reduced expression for the second-order hyperpolarizability is very similar to the residue approach based on quadratic response functions, and as such, it can be viewed as a sum of products of two-photon transition elements from the initial ground to the final excited states. As we approach a one-photon resonance, the intermediate state is a true rather than a virtual state and

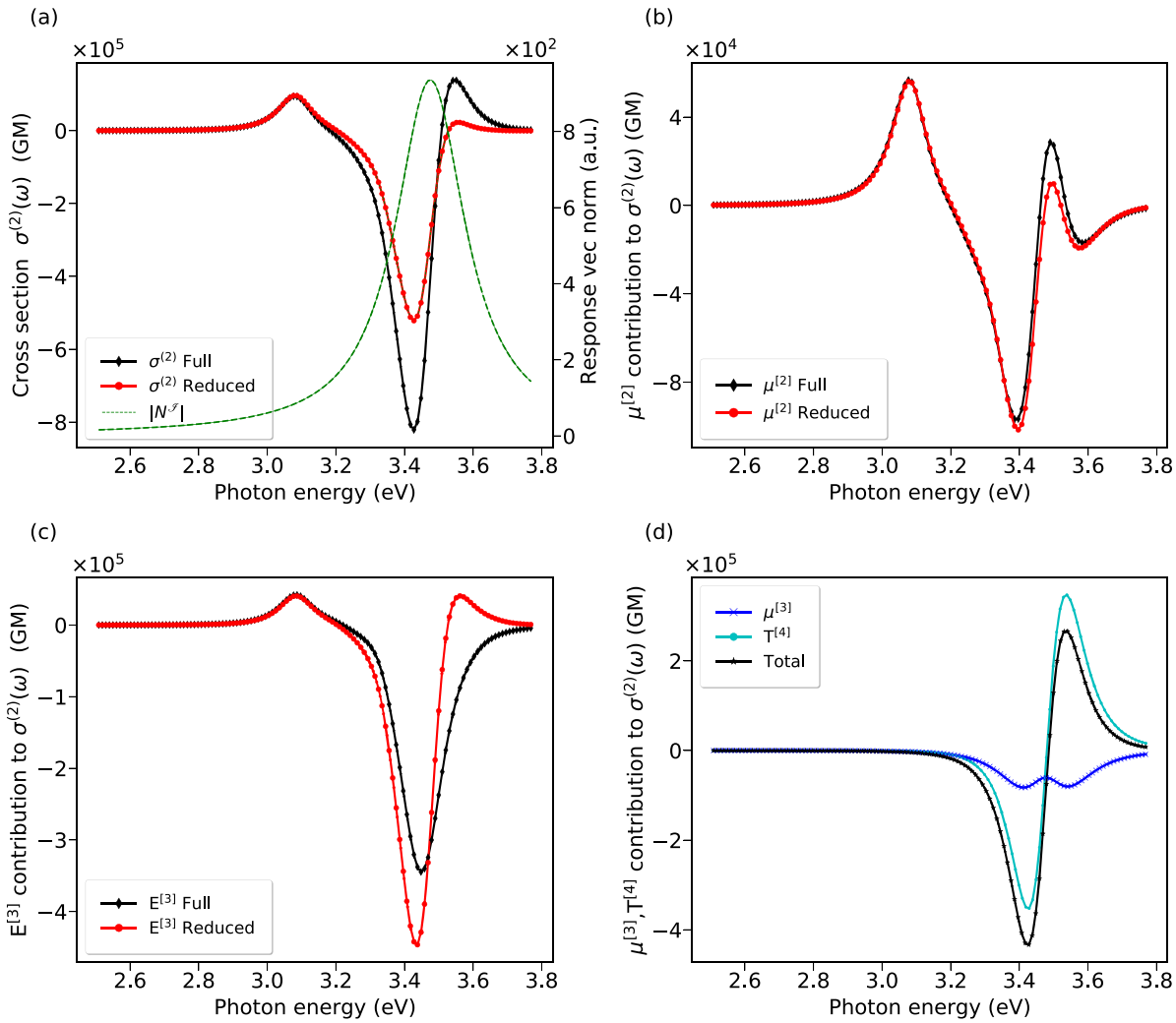

FIG. 3. Two-photon absorption spectra of BPVB in the resonance region at the HF/def2-SVPD level of theory: (a) total two-photon absorption cross section $\sigma^{(2)}$. The total magnitude of the imaginary component of the first-order response vectors $|N^{\mathcal{I}}| = \sum_{\alpha}^{x,y,z} |N_{\alpha}^{\mathcal{I}}|$, (b) contributions to $\sigma^{(2)}$ from $\mu^{[2]}$, (c) contributions to $\sigma^{(2)}$ from $E^{[3]}$, and (d) contributions to $\sigma^{(2)}$ from $T^{[4]}$ and $\mu^{[3]}$.

the TPA cross section now includes contributions from inter-excited state transition elements. These, in turn, appear in the $T^{[4]}$, $\mu^{[3]}$, and $E^{[3]}$ contributions related to the second-order response vectors of $N^{(\lambda+\tau)}$ terms and are omitted in the reduced expression in order to gain computational efficiency in the off-resonance regions. This effect is clearly seen in Fig. 6. As we approach a photon frequency of 5.2 eV, the $T^{[4]}$ and $\mu^{[3]}$ contributions together with the terms in $E^{[3]}$ that are not included in the reduced expression start to dominate the TPA spectrum.

D. Assessment of the reduced form TPA expression

In order to further assess the accuracy of the reduced form expression of the TPA cross section, we have performed a benchmark investigation involving a set of 24 molecules. This set includes small- and medium-sized molecules that are of biochemical interest or being used as building blocks in two-photon material design. For the design of organic two-photon materials, it is well known that π-conjugated push–pull systems are of particular interest. These are divided into the sub-classes of di-, quadru-, and octopolar systems, typically created by variations of terminal donor (D) and acceptor (A) groups.[60] It has been demonstrated that the length of the π-conjugated backbone and the molecular symmetry play key roles for the two-photon activity.[61] Our benchmark set of molecules therefore includes systems spanning the chemical space in these directions.

Specifically, symmetric conjugated push–pull systems with terminal A/D groups change their quadruple moment upon excitation

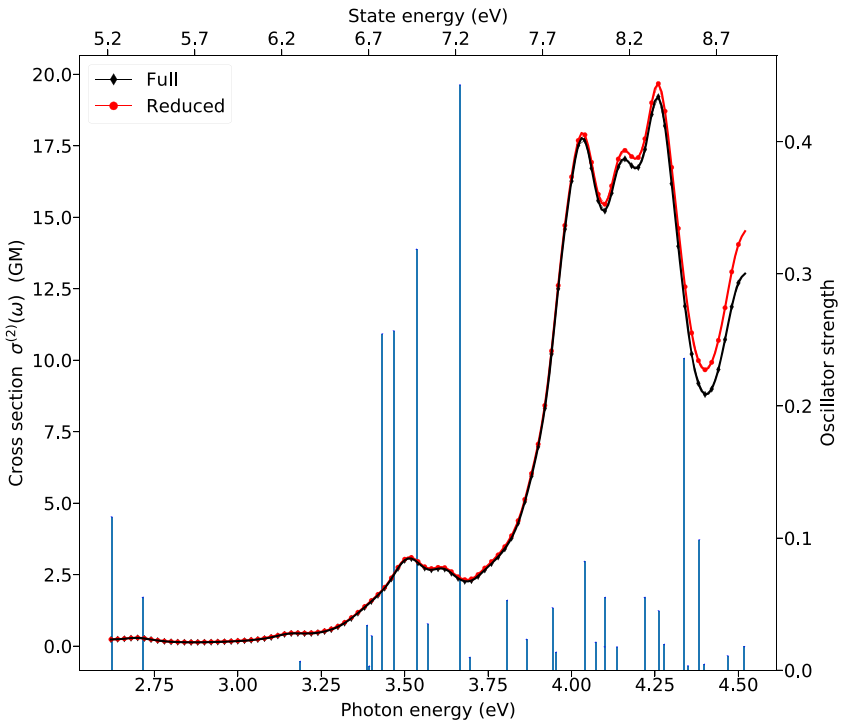

FIG. 4. Oscillator strengths (bars) for the 30 lowest excited states of Ala–Trp and the corresponding TPA spectrum calculated using the full (black) and reduced (red) expressions for the isotropic second-order hyperpolarizability. The results are obtained at the HF/def2-SVPD level of theory.

as to result in large second-order hyperpolarizabilites.[62] Belonging to this class and included in our study, 2,5-di(pyridin-4-yl)thiophene is a symmetric A–π–A system with a π-electron rich thiophene core attached to two pyridine acceptor groups; 5,5′-di(pyridin-4-yl)-2,2′-bithiophene is a symmetric A–π–A system with a longer conjugated core; 4,6-bis((E)-4-(diethylamino)styryl)pyrimidin-2-ol is a symmetric D–π–D system that has been used as a two-photon probe for the bio-imaging of enzymes.[63]

Asymmetric dipolar push–pull systems of the form D–π–A have been shown to possess changes in dipole moment between the ground and excited states, which, in turn, can yield a large nonlinear second-order hyperpolarizability.[62] The rigidity of the π-electron core has also been shown to enhance the nonlinear second-order hyperpolarizability. This can be seen by comparing fluorene and biphenyl as π-electron cores, where the latter has a single bond that can rotate and break the conjugation.[64] As a representative dipolar push–pull system, we have chosen 4-(7-(thiophen-2-yl)-9H-fluoren-2-yl)pyridine that is a small dipolar system with a thiophene donor group, a fluorene π-core, and a pyridine acceptor group as well as *para*-nitroanline (PNA). We have also included the octupolar push–pull system nitrilotris(hepta-2,4,6-trienenitrile).

In regard to state selection, we consider only valence-excited states below the first ionization edge. We further limit the study to include only states with significant TPA cross sections and for which the photon energies, i.e., $\hbar\omega_{f0}/2$, are detuned with respect to the corresponding lowest one-photon transition by at least three times the γ-broadening parameter or some 0.37 eV. In Fig. 7, we show the discrepancies between TPA cross sections at resonant energies, i.e., $\sigma^{(2)}(\omega_{f0}/2)$, as obtained with the full [Eq. (14)] and reduced [Eq. (115)] expressions, and we do so for the several two-photon transitions that pass the selection criteria for each of the 24 molecules in the benchmark set. As shown in Eqs. (107)–(114), the validity of approximating the full expression with the reduced one critically depends on the laser detuning compared to the γ-broadening. The magnitude of an element of the imaginary component of the first-order response vectors has a Lorentzian profile shape as seen from Eq. (106), and it is therefore expected to reduce to one tenth of its maximum value at a detuning of $\hbar(\omega_{10} - \omega) = 3\hbar\gamma = 0.37$ eV. As shown in Fig. 7, there is a clear trend of reduced relative errors with increased laser detuning. Not surprisingly, the molecules showing the largest relative errors were those with two-photon active states with a small laser detuning for which the corresponding $S_0 \leftarrow S_1$ one-photon transition was very strong. With all states and all molecules considered, the relative error remained below 16%, and with a laser detuning of at least 1.0 eV, the error is throughout less than 5%. For the purpose of two-photon material screening and design, we can thus recommend the use of the approximate form of the expression for the hyperpolarizability as errors of some 10% in TPA cross sections are of minor or no concern.

E. Computational efficiency in cubic response TPA calculations

The two key points to consider when assessing the computational efficiency in implementations of SCF response theory are the

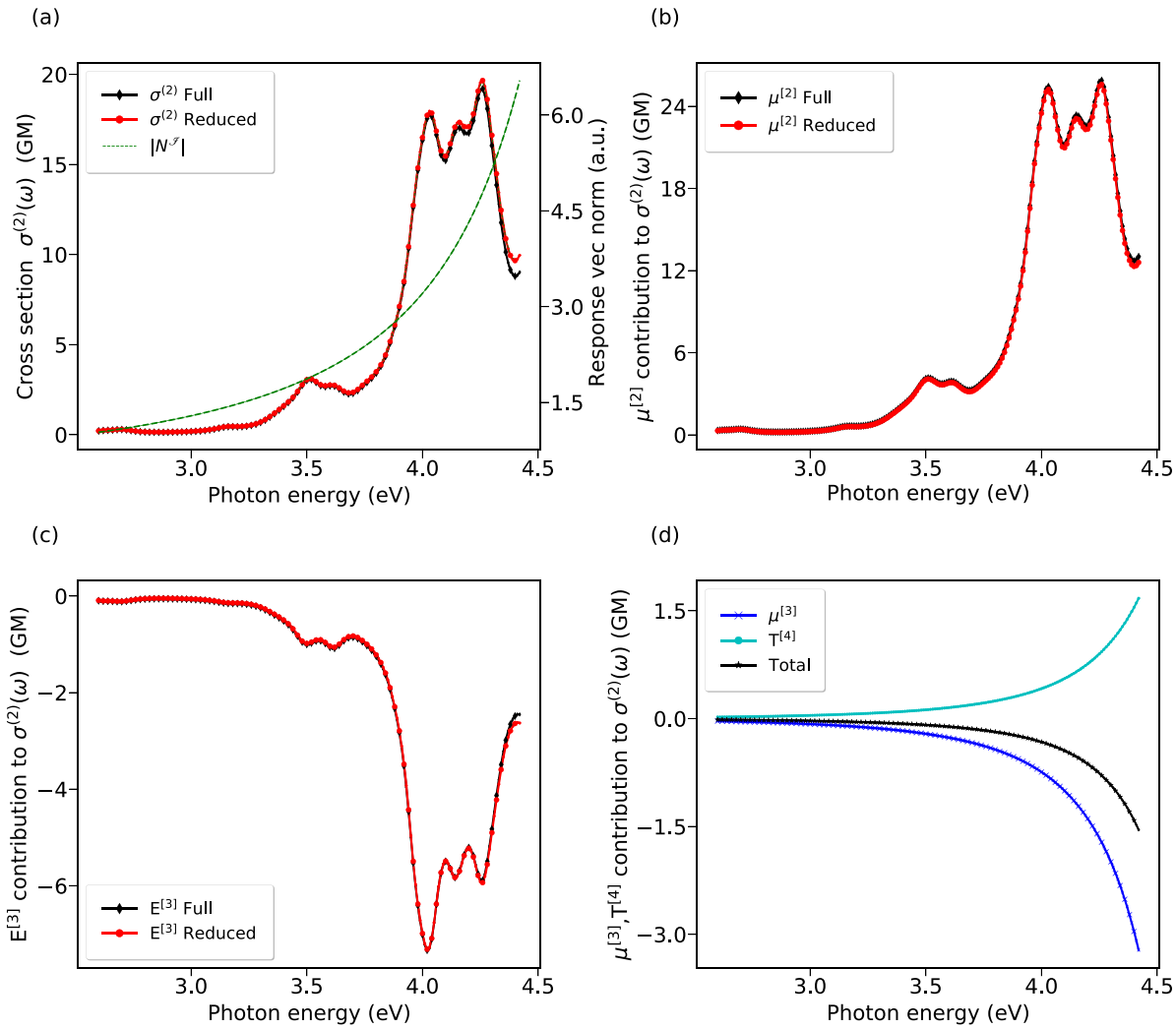

FIG. 5. Two-photon absorption spectra of Ala–Trp in the off-resonance region at the HF/def2-SVPD level of theory: (a) total two-photon absorption cross section $\sigma^{(2)}$. The total magnitude of the imaginary component of the first-order response vectors $|N^{\mathcal{I}}| = \sum_{\alpha}^{x,y,z} |N_{\alpha}^{\mathcal{I}}|$, (b) contributions to $\sigma^{(2)}$ from $\mu^{[2]}$, (c) contributions to $\sigma^{(2)}$ from $E^{[3]}$, and (d) contributions to $\sigma^{(2)}$ from $T^{[4]}$ and $\mu^{[3]}$.

number of auxiliary Fock matrices that need to be constructed and the extent to which these constructions can be made in parallel by supplying multiple auxiliary density matrices to the program module constructing the Fock matrix. As a benchmark, we choose the calculation of the TPA spectrum of Ala–Trp in the optical region between 2.5 eV and 4.5 eV with a frequency grid point separation such that a total of 100 frequencies are employed in the spectrum calculation. We consider the full [Eq. (14)] and the reduced [Eq. (115)] forms for the calculations of the needed isotropic complex second-order hyperpolarizability, $\overline{\gamma}(-\omega;\omega,-\omega,\omega)$. Our calculations are performed on ten standard cluster nodes (Intel Xeon Gold 6130, 32 cores, 96 GB) with a hybrid MPI/OpenMP parallelization scheme for the construction of Fock matrices.

1. Step 1

The first step of the calculation is to obtain the first-order complex response vectors in Eq. (8) for each of the three Cartesian axes $\{x, y, z\}$. As there is a relation between response vectors related with positive and negative frequencies [Eq. (26)], we need only to consider the set of positive frequencies in the calculation and there are thus a total of 300 first-order complex response vectors to be determined. We perform this part of the calculation in both the full and reduced approaches, and the complex linear response equation solver converges the entire set of 300 response vectors in a mere eight iterations with a final dimension of the reduced subspace that is as small as 156. The underlying reason for this remarkably small

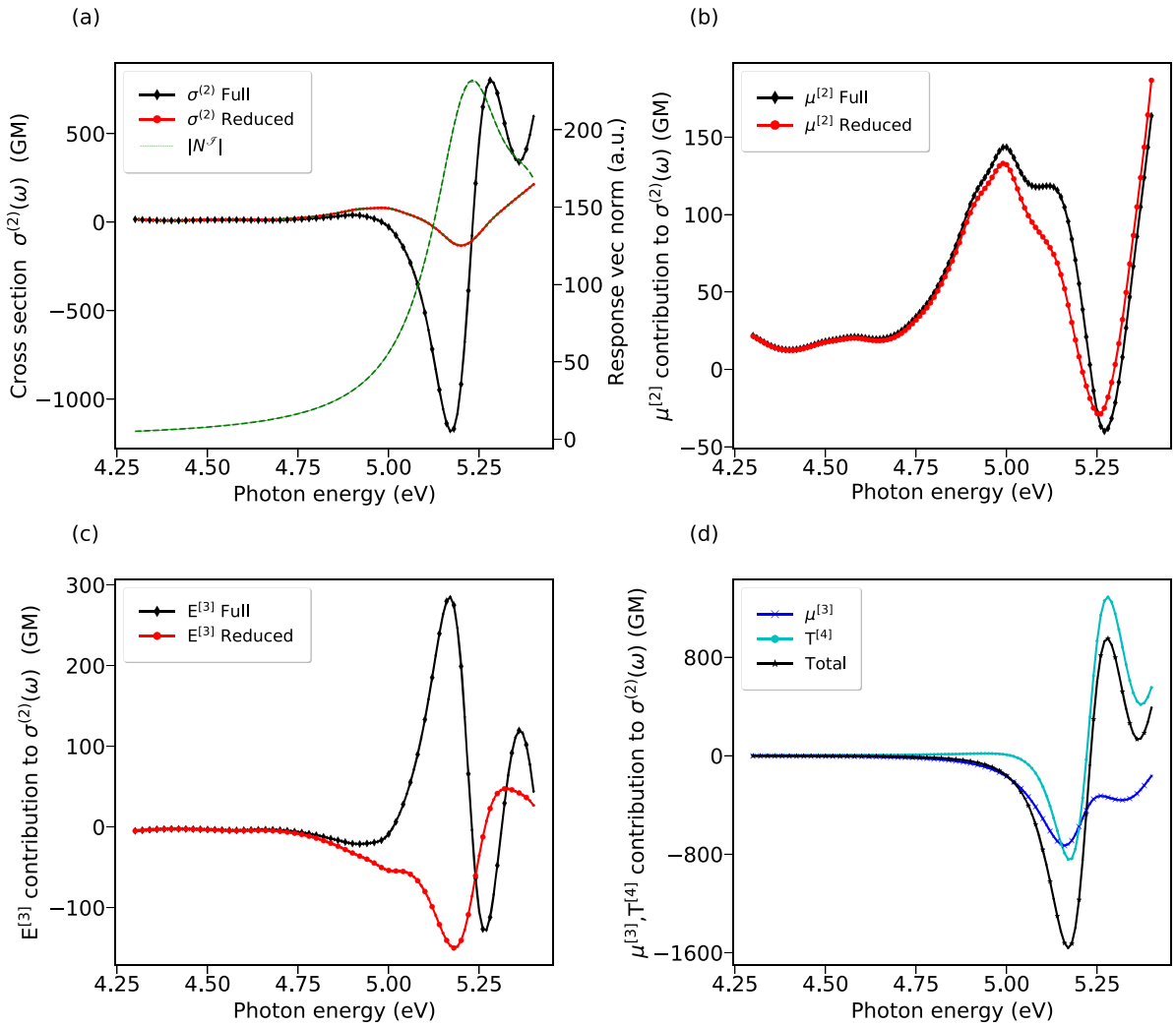

FIG. 6. Two-photon absorption spectra of Ala–Trp in the resonance region at the HF/def2-SVPD level of theory: (a) total two-photon absorption cross section $\sigma^{(2)}$. The total magnitude of the imaginary component of the first-order response vectors $|N^{\mathcal{I}}| = \sum_{\alpha}^{x,y,z} |N_{\alpha}^{\mathcal{I}}|$, (b) contributions to $\sigma^{(2)}$ from $\mu^{[2]}$, (c) contributions to $\sigma^{(2)}$ from $E^{[3]}$, and (d) contributions to $\sigma^{(2)}$ from $T^{[4]}$ and $\mu^{[3]}$.

dimension of the common subspace for the entire set of complex response vectors is the lack of one-photon resonances in this region and the large degree of linear dependence between the resulting response vectors. This part of the calculation finishes in a wall time of 4 min.

2. Step 2

Once the 300 first-order response vectors are available, the second step in the calculation can be performed. This step involves the calculation of 2400 two-time transformed first-order Fock matrices F^{σ} in Eq. (57) and $F^{(\lambda+\tau)}$ in Eq. (64), which are used to construct the 600 second-order complex gradients Λ^{σ} in Eq. (89) and an equal number of $\Lambda^{(\lambda+\tau)}$ in Eq. (92). We note that these Fock matrices are also later reused for the $E^{[4]}$-tensor contraction in Eq. (70).

When employing the reduced form, the number of Fock matrices is halved owing to the fact that the $N^{(\lambda+\tau)}$ vectors do not significantly contribute in the one-photon off-resonance regions, as seen from Eq. (104). The number of Fock matrices is then halved again since the imaginary components of the first-order response vectors are small and can be neglected in this region. The first-order Fock matrices can thus be approximated with only the real component of the 600 F^{σ} matrices of Eq. (57).

The second step of the calculation also involves the calculation of the 600 three-time transformed first-order Fock matrices $F^{(\lambda\sigma\tau)}$ in Eq. (65). These are exclusively used for the $E^{[4]}$-tensor contraction

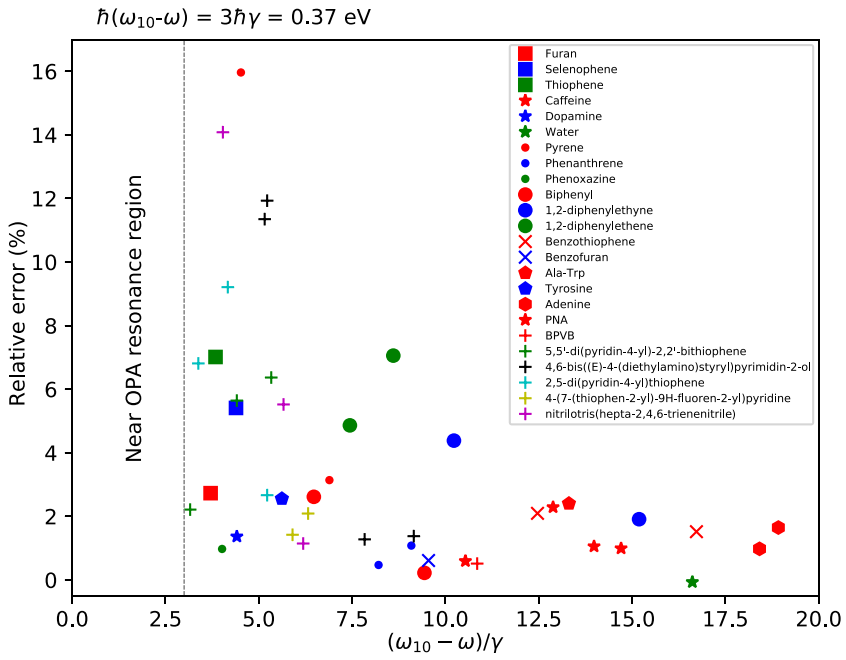

FIG. 7. Relative errors for the low-lying two-photon transitions in the benchmark set of 24 molecules. The results are obtained at the HF/def2-SVP level of theory.

in Eq. (70) and are therefore only calculated when considering the full form of the hyperpolarizability. This is understood since all first-order response vectors are approximately real in the one-photon off-resonance region, and so, the imaginary parts of $E^{[4]}$-terms are negligible. Consequently, the three-time transformed first-order Fock matrices $F^{(\lambda\sigma\tau)}$ need not be calculated in this case.

As a technical remark, we note that the calculation of the 3000 Fock matrices in the second step of the calculation (using the full form) was conducted in two batches due to memory limitation on the compute nodes and every batch requires one calculation of the full set of ERIs. The second step in the calculation was completed within wall times of 71 min and 13 min when employing the full and reduced forms, respectively.

3. Step 3

With access to the compounded second-order gradients, the third step in the calculation involves the calculation of the corresponding 1200 second-order response vectors N^{σ} in Eq. (83) and the same number of response vectors $N^{(\lambda+\tau)}$ in Eq. (82). Convergence for all 2400 response vectors in the iterative linear response equation solver is in this case reached after eight iterations, resulting in a final subspace dimension of 1882. Despite the facts that the second-order response vectors are much less linearly dependent than the first-order ones and the optical second-harmonic frequency in Eq. (83) is in resonance with the transition frequencies of the two-photon states, we observe a convergence of all linear response equations with less than one trial vector per response vector. When employing the reduced form of the expression for the hyperpolarizability, there are only 600 second-order response equations to be solved and the final subspace dimension becomes in this case equal to 1037. The third step in the calculation is completed within wall times of 60 min and 28 min when employing the full and reduced forms, respectively.

4. Step 4

With access to the second-order response vectors, the $E^{[3]}$-tensor contraction in Eq. (15) can be performed. For this, an additional 600 compounded two-time transformed second-order Fock matrices $F^{\lambda,\sigma\tau}$ as defined in Eq. (99) are required to evaluate the total $E^{[3]}$-contribution to the hyperpolarizability as provided in Eq. (93).

The second-order response vectors N^{σ} are resonant in the two-photon spectral region, as seen in Eq. (105), and they will have both real and imaginary parts that are significant. In turn, this implies that the second-order two-time transformed Fock matrices $F^{\lambda,\sigma\tau}$ in Eq. (99) will need to be determined in both the full and reduced forms of the expressions for the isotropic hyperpolarizability. With three Cartesian axes, 100 optical frequencies, and independent real and imaginary parts, this adds a need for the calculation of 600 Fock matrices in the fourth step of the calculation, which was completed within a wall time of 13 min.

5. In total

Using the reduced form of the expression for the isotropic complex second-order hyperpolarizability in the one-photon off-resonance regions provides a substantial reduction in the computational effort. As can be seen in Table II, the use of the reduced form leads to a reduction in the number of first-order Fock matrices by 80% in comparison to the full form, which translated to a reduction in the wall time for this part of the calculation by 79%. In practical applications, we note that the drastically reduced memory footprint is equally important and the example calculation of a

TABLE II. Number of Fock matrices and wall time (in minutes) required for the calculation of the UV/vis TPA spectrum for Ala–Trp in the region of 2.5 eV–4.5 eV (adopting 100 frequency grid points and a damping parameter of 0.12 eV). The calculation employs the def2-SVPD basis set (545 contracted basis functions) and is performed on ten standard cluster nodes (Intel Xeon Gold 6130, 32 cores, 96 GB) with a hybrid MPI/OpenMP parallelization scheme for the construction of Fock matrices.

	Algorithm C			
	Full		Reduced	
	Fock matrices	Wall time	Fock matrices	Wall time
Linear response equation solver				
First-order response vectors	156	4	156	4
Second-order response vectors	1882	60	1037	28
Tensor contractions				
First-order Fock matrices				
Λ-gradients	2400	...	600	...
$E^{[4]}$-contractions	600	...	0	...
	3000	71	600	13
Second-order Fock matrices				
$E^{[3]}$-contractions	600	14	600	13
Total	5638	150	2393	58

medium-sized system using an appropriate basis set for nonlinear response property calculations is completed within a wall time of 1 h on ten standard cluster nodes.

For comparison, the calculation of a TPA spectrum over a spectral region covered by 100 frequency grid-points using the γ-tensor component method (Algorithm A) would require an astonishing 36 600 first- and second-order Fock matrices. In the present work, we have reduced this number to 3600 and 1200 using, respectively, the full and reduced forms of the γ-tensor average method (Algorithm C).

IV. SUMMARY

Computationally tractable expressions for the calculation of TPA spectra from the imaginary part of the second-order hyperpolarizability have been derived and implemented using the complex polarization propagator approach to cubic order in perturbation theory. The present work adopts the Hartree–Fock approximation with Fock-matrix driven handling of the contractions of second-, third-, and fourth-order generalized Hessian matrices with trial and first- and second-order response vectors.

We have demonstrated a highly efficient algorithm for obtaining TPA cross sections for randomly oriented systems where the isotropic γ-tensor is put in computational focus without explicit reference to individual tensor components. The presented tensor-average algorithm introduces compound Fock matrices and response vectors, and without the introduction of approximations, TPA cross sections are determined with a mere 10% of the number of unique Fock matrices required in the tensor-component approach. With the introduction of physically well motivated approximations in one-photon off-resonance regions of the spectrum, the number of Fock matrices in the calculation has been further reduced by a factor of three. The error in the TPA cross section as introduced by these approximations is shown to be negligible in example calculations on the dipeptide alanine–tryptophan and the two-photon chromophore 5-dibromo-1,4-bis(2-(4-diphenylaminophenyl)vinyl)-benzene as well as for a wider benchmark study.

In contrast to conventional calculations of TPA moments from residues of quadratic-response functions, the cubic-response approach is perfectly applicable to systems with a high density of states. Combined with the fact that the presented novel reduced-form algorithm largely removes central processing unit (CPU) and memory bottlenecks associated with cubic-response based TPA calculations, we argue that our work will be important so as to enable TPA spectrum simulations for large-scale systems of real technical interest. Before reaching this point, however, it is imperative to extend the present work to the level of DFT. Since the exchange–correlation kernels are nonlinear, the constructions of compound Fock matrices will not directly apply to the corresponding Kohn–Sham matrices. However, we expect the Coulomb and exact exchange contributions treated in the present work to dominate the overall computational cost so that a more expensive approach can be afforded for the exchange–correlation contributions. This will be the study of future work.

ACKNOWLEDGMENTS

Financial support is acknowledged from the European Commission in the form of the ITN titled *Computational Spectroscopy in Natural Sciences and Engineering* (COSINE) (Grant No. 765739), the Swedish e-Science Research Centre (SeRC), and the Swedish Research Council (Grant No. 2018-4343). Computational resources are provided by the Swedish National Infrastructure for Computing (SNIC).

DATA AVAILABILITY

The data that support the findings of this study are available from the corresponding author upon reasonable request.

REFERENCES

[1] M. Göppert-Mayer, Ann. Phys. **401**, 273 (1931).
[2] M. Deubel, G. Von Freymann, M. Wegener, S. Pereira, K. Busch, and C. M. Soukoulis, Nat. Mater. **3**, 444 (2004).
[3] M. Carlotti and V. Mattoli, Small **15**, 1902687 (2019).
[4] S. Wu, J. Serbin, and M. Gu, J. Photochem. Photobiol., A **181**, 1 (2006).
[5] C. A. Coenjarts and C. K. Ober, Chem. Mater. **16**, 5556 (2004).
[6] W. R. Zipfel, R. M. Williams, and W. W. Webb, Nat. Biotechnol. **21**, 1369 (2003).
[7] W. D. F. Helmchen, Nat. Methods **2**, 932 (2005).
[8] B. N. Ozbay, G. L. Futia, M. Ma, V. M. Bright, J. T. Gopinath, E. G. Hughes, D. Restrepo, and E. A. Gibson, Sci. Rep. **8**, 8108 (2018).
[9] H.-Y. Ahn, K. E. Fairfull-Smith, B. J. Morrow, V. Lussini, B. Kim, M. V. Bondar, S. E. Bottle, and K. D. Belfield, J. Am. Chem. Soc. **134**, 4721 (2012).
[10] F. Bolze, S. Jenni, A. Sour, and V. Heitz, Chem. Commun. **53**, 12857 (2017).
[11] K. Ogawa and Y. Kobuke, Biomed Res. Int. **2013**, 1 (2012).
[12] C. Tang, Q. Zheng, H. Zhu, L. Wang, S.-C. Chen, E. Ma, and X. Chen, J. Mater. Chem. C **1**, 1771 (2013).
[13] Q. Li, C. Liu, Z. Liu, and Q. Gong, Opt. Express **13**, 1833 (2005).
[14] D. A. Parthenopoulos and P. M. Rentzepis, Science **245**, 843 (1989).
[15] A. Specht, F. Bolze, L. Donato, C. Herbivo, S. Charon, D. Warther, S. Gug, J.-F. Nicoud, and M. Goeldner, Photochem. Photobiol. Sci. **11**, 578 (2012).
[16] A. Y. Vorobev and A. E. Moskalensky, Comput. Struct. Biotechnol. J. **18**, 27 (2020).
[17] A. Herrmann, Photochem. Photobiol. Sci. **11**, 446 (2012).
[18] R. H. Kramer, J. J. Chambers, and D. Trauner, Nat. Chem. Biol. **1**, 360 (2005).
[19] H.-M. Lee, D. R. Larson, and D. S. Lawrence, ACS Chem. Biol. **4**, 409 (2009).
[20] C.-C. Lin and K. S. Anseth, Pharm. Res. **26**, 631 (2009).
[21] M. Goeldner and R. G. Eds, in *Dynamic Studies in Biology*, edited by M. Goeldner and R. S. Givens (Wiley, 2005), pp. 435–459.
[22] D. Puliti, D. Warther, C. Orange, A. Specht, and M. Goeldner, Bioorg. Med. Chem. **19**, 1023 (2011).
[23] Y. Shigeri, Y. Tatsu, and N. Yumoto, Pharmacol. Ther. **91**, 85 (2001).
[24] H. Zhao, E. S. Sterner, E. B. Coughlin, and P. Theato, Macromolecules **45**, 1723 (2012).
[25] Y. Zhang, N. Luan, K. Li, J. Leng, and W. Hu, Sensors **20**, 1760 (2020).
[26] E. Dalgaard, Phys. Rev. A **26**, 42 (1982).
[27] J. Olsen and P. Jørgensen, J. Chem. Phys. **82**, 3235 (1985).
[28] P. Norman, D. M. Bishop, H. J. A. Jensen, and J. Oddershede, J. Chem. Phys. **115**, 10323 (2001).
[29] P. Norman, D. M. Bishop, H. J. A. Jensen, and J. Oddershede, J. Chem. Phys. **123**, 194103 (2005).
[30] P. Norman, Phys. Chem. Chem. Phys. **13**, 20519 (2011).
[31] P. Norman, K. Ruud, and T. Saue, *Principles and Practices of Molecular Properties* (John Wiley & Sons, Ltd., Chichester, UK, 2018).
[32] P. Norman, D. Jonsson, O. Vahtras, and H. Ågren, Chem. Phys. **203**, 23 (1996).
[33] P. Norman, D. Jonsson, H. Ågren, P. Dahle, K. Ruud, T. Helgaker, and H. Koch, Chem. Phys. Lett. **253**, 1 (1996).
[34] D. Jonsson, P. Norman, and H. Ågren, J. Chem. Phys. **105**, 6401 (1996).
[35] T. Fahleson, H. Ågren, and P. Norman, J. Phys. Chem. Lett. **7**, 1991 (2016).
[36] T. Fahleson and P. Norman, J. Chem. Phys. **147**, 144109 (2017).
[37] K. Aidas, C. Angeli, K. L. Bak, V. Bakken, R. Bast, L. Boman, O. Christiansen, R. Cimiraglia, S. Coriani, P. Dahle, E. K. Dalskov, U. Ekström, T. Enevoldsen, J. J. Eriksen, P. Ettenhuber, B. Fernández, L. Ferrighi, H. Fliegl, L. Frediani, K. Hald, A. Halkier, C. Hättig, H. Heiberg, T. Helgaker, A. C. Hennum, H. Hettema, E. Hjertenaes, S. Høst, I.-M. Høyvik, M. F. Iozzi, B. Jansík, H. J. A. Jensen, D. Jonsson, P. Jørgensen, J. Kauczor, S. Kirpekar, T. Kjaergaard, W. Klopper, S. Knecht, R. Kobayashi, H. Koch, J. Kongsted, A. Krapp, K. Kristensen, A. Ligabue, O. B. Lutnaes, J. I. Melo, K. V. Mikkelsen, R. H. Myhre, C. Neiss, C. B. Nielsen, P. Norman, J. Olsen, J. M. H. Olsen, A. Osted, M. J. Packer, F. Pawlowski, T. B. Pedersen, P. F. Provasi, S. Reine, Z. Rinkevicius, T. A. Ruden, K. Ruud, V. V. Rybkin, P. Sałek, C. C. M. Samson, A. S. de Merás, T. Saue, S. P. A. Sauer, B. Schimmelpfennig, K. Sneskov, A. H. Steindal, K. O. Sylvester-Hvid, P. R. Taylor, A. M. Teale, E. I. Tellgren, D. P. Tew, A. J. Thorvaldsen, L. Thøgersen, O. Vahtras, M. A. Watson, D. J. D. Wilson, M. Ziolkowski, and H. Ågren, Wiley Interdiscip. Rev.: Comput. Mol. Sci. **4**, 269 (2014).
[38] P. Sałek, O. Vahtras, J. Guo, Y. Luo, T. Helgaker, and H. Ågren, Chem. Phys. Lett. **374**, 446 (2003).
[39] H. Hettema, H. J. A. Jensen, P. Jørgensen, and J. Olsen, J. Chem. Phys. **97**, 1174 (1992).
[40] C. Hättig, O. Christiansen, and P. Jørgensen, J. Chem. Phys. **108**, 8355 (1998).
[41] F. Furche, R. Ahlrichs, C. Hättig, W. Klopper, M. Sierka, and F. Weigend, Wiley Interdiscip. Rev.: Comput. Mol. Sci. **4**, 91 (2014).
[42] S. M. Parker, D. Rappoport, and F. Furche, J. Chem. Theory Comput. **14**, 807 (2018).
[43] A. S. P. Gomes, T. Saue, L. Visscher, H. J. A. Jensen, and R. Bast, with contributions from I. A. Aucar, V. Bakken, K. G. Dyall, S. Dubillard, U. Ekström, E. Eliav, T. Enevoldsen, E. Faßhauer, T. Fleig, O. Fossgaard, L. Halbert, E. D. Hedegård, B. Heimlich-Paris, T. Helgaker, J. Henriksson, M. Iliaš, C. R. Jacob, S. Knecht, S. Komorovský, O. Kullie, J. K. Lærdahl, C. V. Larsen, Y. S. Lee, H. S. Nataraj, M. K. Nayak, P. Norman, G. Olejniczak, J. Olsen, J. M. H. Olsen, Y. C. Park, J. K. Pedersen, M. Pernpointner, R. di Remigio, K. Ruud, P. Sałek, B. Schimmelpfennig, B. Senjean, A. Shee, J. Sikkema, A. J. Thorvaldsen, J. Thyssen, J. van Stralen, M. L. Vidal, S. Villaume, O. Visser, T. Winther, and S. Yamamoto (2019). "DIRAC, a relativistic *ab initio* electronic structure program, release DIRAC19," Zenodo. https://doi.org/10.5281/zenodo.3572669; see also http://www.diracprogram.org.
[44] J. Henriksson, P. Norman, and H. J. A. Jensen, J. Chem. Phys. **122**, 114106 (2005).
[45] J. Henriksson, T. Saue, and P. Norman, J. Chem. Phys. **128**, 024105 (2008).
[46] Y. Shao, Z. Gan, E. Epifanovsky, A. T. B. Gilbert, M. Wormit, J. Kussmann, A. W. Lange, A. Behn, J. Deng, X. Feng, D. Ghosh, M. Goldey, P. R. Horn, L. D. Jacobson, I. Kaliman, R. Z. Khaliullin, T. Kuś, A. Landau, J. Liu, E. I. Proynov, Y. M. Rhee, R. M. Richard, M. A. Rohrdanz, R. P. Steele, E. J. Sundstrom, H. L. Woodcock III, P. M. Zimmerman, D. Zuev, B. Albrecht, E. Alguire, B. Austin, G. J. O. Beran, Y. A. Bernard, E. Berquist, K. Brandhorst, K. B. Bravaya, S. T. Brown, D. Casanova, C.-M. Chang, Y. Chen, S. H. Chien, K. D. Closser, D. L. Crittenden, M. Diedenhofen, R. A. DiStasio, Jr., H. Do, A. D. Dutoi, R. G. Edgar, S. Fatehi, L. Fusti-Molnar, A. Ghysels, A. Golubeva-Zadorozhnaya, J. Gomes, M. W. D. Hanson-Heine, P. H. P. Harbach, A. W. Hauser, E. G. Hohenstein, Z. C. Holden, T.-C. Jagau, H. Ji, B. Kaduk, K. Khistyaev, J. Kim, J. Kim, R. A. King, P. Klunzinger, D. Kosenkov, T. Kowalczyk, C. M. Krauter, K. U. Lao, A. D. Laurent, K. V. Lawler, S. V. Levchenko, C. Y. Lin, F. Liu, E. Livshits, R. C. Lochan, A. Luenser, P. Manohar, S. F. Manzer, S.-P. Mao, N. Mardirossian, A. V. Marenich, S. A. Maurer, N. J. Mayhall, E. Neuscamman, C. M. Oana, R. Olivares-Amaya, D. P. O'Neill, J. A. Parkhill, T. M. Perrine, R. Peverati, A. Prociuk, D. R. Rehn, E. Rosta, N. J. Russ, S. M. Sharada, S. Sharma, D. W. Small, A. Sodt, T. Stein, D. Stück, Y.-C. Su, A. J. W. Thom, T. Tsuchimochi, V. Vanovschi, L. Vogt, O. Vydrov, T. Wang, M. A. Watson, J. Wenzel, A. White, C. F. Williams, J. Yang, S. Yeganeh, S. R. Yost, Z.-Q. You, I. Y. Zhang, X. Zhang, Y. Zhao, B. R. Brooks, G. K. L. Chan, D. M. Chipman, C. J. Cramer, W. A. Goddard III, M. S. Gordon, W. J. Hehre, A. Klamt, H. F. Schaefer III, M. W. Schmidt, C. D. Sherrill, D. G. Truhlar, A. Warshel, X. Xu, A. Aspuru-Guzik, R. Baer, A. T. Bell, N. A. Besley, J.-D. Chai, A. Dreuw, B. D. Dunietz, T. R. Furlani, S. R. Gwaltney, C.-P. Hsu, Y. Jung, J. Kong, D. S. Lambrecht, W. Liang, C. Ochsenfeld, V. A. Rassolov, L. V. Slipchenko, J. E. Subotnik, T. Van Voorhis, J. M. Herbert, A. I. Krylov, P. M. W. Gill, and M. Head-Gordon, Mol. Phys. **113**, 184 (2015).
[47] S. Knippenberg, D. R. Rehn, M. Wormit, J. H. Starcke, I. L. Rusakova, A. B. Trofimov, and A. Dreuw, J. Chem. Phys. **136**, 064107 (2012).
[48] M. T. P. Beerepoot, D. H. Friese, N. H. List, J. Kongsted, and K. Ruud, Phys. Chem. Chem. Phys. **17**, 19306 (2015).

[49]D. H. Friese, C. Hättig, and K. Ruud, Phys. Chem. Chem. Phys. **14**, 1175 (2012).
[50]M. J. Paterson, O. Christiansen, F. Pawłowski, P. Jørgensen, C. Hättig, T. Helgaker, and P. Sałek, J. Chem. Phys. **124**, 054322 (2006).
[51]K. D. Nanda and A. I. Krylov, J. Chem. Phys. **142**, 064118 (2015).
[52]K. Kristensen, J. Kauczor, T. Kjærgaard, and P. Jørgensen, J. Chem. Phys. **131**, 044112 (2009).
[53]K. Kristensen, J. Kauczor, A. J. Thorvaldsen, P. Jørgensen, T. Kjærgaard, and A. Rizzo, J. Chem. Phys. **134**, 214104 (2011).
[54]J. Kauczor, P. Jørgensen, and P. Norman, J. Chem. Theory Comput. **7**, 1610 (2011).
[55]J. Kauczor and P. Norman, J. Chem. Theory Comput. **10**, 2449 (2014).
[56]Z. Rinkevicius, X. Li, O. Vahtras, K. Ahmadzadeh, M. Brand, M. Ringholm, N. H. List, M. Scheurer, M. Scott, A. Dreuw, and P. Norman, Wiley Interdiscip. Rev.: Comput. Mol. Sci. **10**, e1457 (2020).
[57]P. Norman, D. Jonsson, O. Vahtras, and H. Ågren, Chem. Phys. Lett. **242**, 7 (1995).
[58]S. Grimme, C. Bannwarth, and P. Shushkov, J. Chem. Theory Comput. **13**, 1989 (2017).
[59]M. Albota, D. Beljonne, J. L. Brédas, J. Ehrlich, J. Fu, A. Heikal, S. Hess, T. Kogej, M. Levin, S. Marder, D. McCord-Maughon, J. Perry, H. Röckel, M. Rumi, G. Subramaniam, W. Webb, X. Wu, and C. Xu, Science **281**, 1653 (1998).
[60]G. S. He, L.-S. Tan, Q. Zheng, and P. N. Prasad, Chem. Rev. **108**, 1245 (2008).
[61]L. Antonov, K. Kamada, K. Ohta, and F. S. Kamounah, Phys. Chem. Chem. Phys. **5**, 1193 (2003).
[62]X. M. Wang, D. Wang, G. Y. Zhou, W. T. Yu, Y. F. Zhou, Q. Fang, and M. H. Jiang, J. Mater. Chem. **11**, 1600 (2001).
[63]L. Qian, L. Li, and S. Q. Yao, Acc. Chem. Res. **49**, 626 (2016).
[64]P. Prabhakaran, T. D. Kim, and K. S. Lee, *Polymer Science: A Comprehensive Reference, 10 Volume Set* (Elsevier B.V., 2012), Vol. 8, pp. 211–260.